

AD-A253 416



(2)

OFFICE OF NAVAL RESEARCH

Grant N00014-90-J-1193

TECHNICAL REPORT No. 88

Temperature Variation of the Elementary Excitation Spectrum of Thin Liquid ^4He Films

by

Chung-In Um, Sang-Tahk Nam, Soo-Young Lee and Thomas F. George

Prepared for publication

in

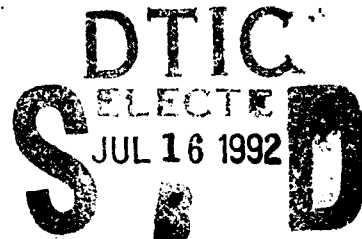
Physical Review B

Departments of Chemistry and Physics
Washington State University
Pullman, WA 99164-1046

July 1992

Reproduction in whole or in part is permitted for any purpose of the United States Government.

This document has been approved for public release and sale; its distribution is unlimited.



92-18849



92 7 15 041

REPORT DOCUMENTATION PAGE

Form Approved
OMB No. 0704-0188

Public reporting burden for this collection of information is estimated to average 1 hour per response, including the time for reviewing instructions, searching existing data sources, gathering and maintaining the data needed, and completing and reviewing the collection of information. Send comments regarding this burden estimate or any other aspect of this collection of information, including suggestions for reducing this burden, to Washington Headquarters Services, Directorate for Information Operations and Reports, 1215 Jefferson Davis Highway, Suite 1204 Arlington, VA 22202-4302, and to the Office of Management and Budget, Paperwork Reduction Project (0704-0188), Washington, DC 20503.

1. AGENCY USE ONLY (Leave blank)		2. REPORT DATE July 1992	3. REPORT TYPE AND DATES COVERED Interim	
4. TITLE AND SUBTITLE Temperature Variation of the Elementary Excitation Spectrum of Thin Liquid ⁴ He Films			5. FUNDING NUMBERS Grant N00014-90-J-1193	
6. AUTHOR(S) Chung-In Um, Sang-Tahk Nam, Soo-Young Lee and Thomas F. George				
7. PERFORMING ORGANIZATION NAME(S) AND ADDRESS(ES) Departments of Chemistry and Physics Washington State University			8. PERFORMING ORGANIZATION REPORT NUMBER WSU/92/88	
9. SPONSORING/MONITORING AGENCY NAME(S) AND ADDRESS(ES) Office of Naval Research 800 N. Quincy Street Arlington, Virginia 22217			10. SPONSORING/MONITORING AGENCY REPORT NUMBER	
11. SUPPLEMENTARY NOTES Prepared for publication in <u>Physical Review B</u>				
12a. DISTRIBUTION / AVAILABILITY STATEMENT Approved for public release; distribution unlimited			12b. DISTRIBUTION CODE	
13. ABSTRACT (Maximum 200 words) The temperature variation of the elementary excitation spectrum of thin liquid ⁴ He films is derived within the ring diagram approximation. This theory is microscopic only in the long wavelength limit. Using this anomalous spectrum, the specific heat data adsorbed on Grafoil graphite and the first, second and third sounds are analyzed. The temperature variation of the phonon spectrum is very negligible for low temperatures. However, with increasing temperature from 0.6 ~ 0.7 K to near the vicinity of the two-dimensional transition temperature of 1.21 K, the temperature effect is significant regarding the physical properties of thin liquid ⁴ He films.				
14. SUBJECT TERMS THIN LIQUID ⁴ He FILMS ELEMENTARY EXCITATION SPECTRUM TEMPERATURE VARIATION SPECIFIC HEAT DATA SECOND AND THIRD SOUNDS LONG WAVELENGTH LIMIT			15. NUMBER OF PAGES 55 16. PRICE CODE NTIS	
17. SECURITY CLASSIFICATION OF REPORT Unclassified	18. SECURITY CLASSIFICATION OF THIS PAGE Unclassified	19. SECURITY CLASSIFICATION OF ABSTRACT Unclassified	20. LIMITATION OF ABSTRACT	

Temperature variation of the elementary excitation spectrum of
thin liquid ^4He films

Chung-In Um, Sang-Tahk Nam and Soo-Young Lee
Department of Physics
College of Science
Korea University, Seoul 136-701, Korea

and

Thomas F. George^{*}
Departments of Chemistry and Physics
Washington State University
Pullman, Washington 99164-1046

The temperature variation of the elementary excitation spectrum of thin liquid ^4He films is derived within the ring diagram approximation. This theory is microscopic only in the long wavelength limit. Using this anomalous spectrum, the specific heat data adsorbed on Grafoil graphite and the first, second and third sounds are analyzed. The temperature variation of the phonon spectrum is very negligible for low temperatures. However, with increasing temperature from 0.6 - 0.7 K to near the vicinity of the two-dimensional transition temperature of 1.21 K, the temperature effect is significant regarding the physical properties of thin liquid ^4He films.

PACS No. 67.40Db, 67.40 Kh, 67.40 Mj, 67.40Pm.

* To whom correspondence should be addressed

Accession For	
NTIS GRA&I	<input checked="" type="checkbox"/>
DTIC TAB	<input type="checkbox"/>
Unannounced	<input type="checkbox"/>
Justification	
By	
Distribution/	
Availability Codes	
Dist	Avail and/or Special
A-1	

I. Introduction

The understanding of elementary excitation spectrums of two- and three-dimensional liquid ^4He has been one of the important problems in low-temperature condensed matter physics. After Landau's well-known phenomenological theory¹ for liquid ^4He , many microscopic theories have been developed by Bogoliubov,² Feynman and Cohen,³ Lee and Yang⁴ and others.⁵ By considering of interactions between quasiparticles, Kebukawa et al and Iwamoto⁶ have tried to explain the multi-excitation spectrum in bulk liquid ^4He . However, most theories have been primarily developed for absolute zero temperature and have yielded the normal dispersion (convex down) relation, which yields the wrong spectrum, whereas the anomalous dispersion (concave up) relation is correct. In the former case, four-phonon processes turn out to be the lowest order, while in the latter case three-phonon processes are the lowest.⁷

Recently Chin and Krotscheck⁸ computed the ground-state structure and collective excitation energies of ^4He droplets at zero temperature, which are described by a generalized Feynman theory, while Krishna and Whaley⁹ calculated the excitation spectra of compressional modes of ^4He for 20, 70 and 240 clusters at 0 K. Chakraborty et al¹⁰ derived the excitation spectrum from the random-phase approximation with the assumption that Bogoliubov excitation is noninteracting, and they found that the spectrum agrees only qualitatively with the experiment. On the other hand, Reppy et al¹² observed sharp cusplike heat capacity singularities in coincidence with the superfluid transition, which is strongly related to the excitation spectrum, and confirmed that ^4He -filled aerogels are not in the same universal class as bulk helium. Stirling et al¹³ performed high-precision neutron scattering measurements of the

temperature dependence of the phonon and roton excitation in liquid ^4He at saturated vapor pressure in both the superfluid and normal-fluid phases.

For two-dimensional liquid ^4He , in recent developments of experimental techniques, the properties of ^4He films have been widely investigated. Some years ago, Isihara and Um¹³ derived successfully the elementary excitation spectrums, that are microscopic only in the long wavelength limit, for two- and three-dimensional liquid ^4He in the zero temperature limit using the ring diagram approximation, which gives anomalous phonon-like behavior at low momenta and roton-like at high momenta. Starting with these elementary excitation, we have successfully explained phonon decay,¹⁴ first,¹⁵ second¹⁶ and third sound,¹⁷ their sound attenuation,¹⁸ thermal conductivity,¹⁹ first viscosity²⁰ and thermal diffusion.²¹

According to the experiments performed by Wood²² and others,²³ it is well known that the temperature variation of the elementary excitation is small but becomes significant in the vicinity of the λ -point. However, we have not found any calculations of this temperature variation in two-dimensional liquid ^4He . All the more, we still do not know whether or not the effect of the temperature variation on three-phonon processes is significant, which is a question not addressed by Landau or Khalatnikov.

It is the purpose of this paper to evaluate the temperature variation of the elementary excitation spectrum of two-dimensional liquid ^4He on the basis of a microscopic theory in the long wavelength limit in the ring diagram approximation, and then to investigate the temperature effect on the structure factor, thermodynamic functions, fluid density and various sounds of two-dimensional liquid ^4He . In Sec. II we shall treat the pair distribution function using the chain diagram approximation and present some basic formulas which will be used in the following sections. The structure factor and the

elementary excitation spectrum will be evaluated in Secs. III and IV, respectively. The thermodynamic functions and fluid densities will be given in Sec. V. We shall evaluate the first, second and third sounds in Sec. VI, and finally in Sec. VII we shall discuss our present results in comparison with related work.

II. Chain diagram approximation

In this section we offer the formula of the pair distribution function within the chain diagram approximation and related formulas and then derive the excitation spectrum in the long wavelength limit at absolute zero temperature. The chain diagram approximation is justified since in a two-dimensional Bose system the pair distribution function depends on the modified Bessel function of order zero, i.e., $K_0(r)$, in contrast to an ideal gas. Within this approximation,²⁴ the pair distribution function $\rho_2(r)$ of a two-dimensional Bose liquid is given as

$$\rho_2(r) = n^2 + I_2(r) - \frac{1}{(2\pi)^2 \beta} \sum_{j=-\infty}^{\infty} \int d\vec{q} \frac{u(q) \lambda_j^2(q)}{1 + u(q) \lambda_j(q)} e^{i\vec{q} \cdot \vec{r}} \quad (2.1)$$

where n is the number density, $\beta = 1/k_B T$, $u(q)$ is the Fourier transform of the interaction potential, λ_j is the j -th eigenvalue of the effective boson propagator representing the unit of a chain, and $I_2(r)$ is the ideal-gas contribution given as

$$I_2(r) = \frac{1}{(2\pi)^4} \int d\vec{p} d\vec{q} f(\vec{p}) f(\vec{p} + \vec{q}) e^{i\vec{p} \cdot \vec{r}} \quad (2.2)$$

The eigenvalues $\lambda_j(q)$ of the effective propagator can be obtained from the expression

$$\lambda_j(q) = \frac{1}{(2\pi)^2} \int_0^\beta d\alpha \int d\vec{p} f(p) [1 + f(\vec{p} + \vec{q})] \exp[\alpha(p^2 - (\vec{p} + \vec{q})^2)] e^{\frac{2\pi i}{\beta} j} , \quad (2.3)$$

where $f(p)$ is the Bose-Einstein distribution function

$$f(p) = \frac{ze^{-\beta p^2}}{1 - ze^{-\beta p^2}} , \quad (2.4)$$

where z is the fugacity.

The integrand of Eq. (2.1) can be divided into two parts as

$$- \sum_j \frac{u(q)\lambda_j^2(q)}{1 + u(q)\lambda_j(q)} = - \sum_j \lambda_j(q) + \frac{\lambda_j(q)}{1 + u(q)\lambda_j(q)} . \quad (2.5)$$

From the definition of $\lambda_j(q)$ in Eq. (2.3), the first term on the right-hand side of Eq. (2.5) yields

$$- \frac{1}{\beta} \sum_j \int \frac{d\vec{q}}{(2\pi)^2} \lambda_j(q) e^{i\vec{q} \cdot \vec{r}} = - n\delta(r) - I_2(r) . \quad (2.6)$$

Hence, the pair distribution function $\rho_2(r)$ becomes

$$\rho_2(r) = n^2 - n\delta(r) + \frac{1}{\beta} \sum_j \frac{d\vec{q}}{(2\pi)^2} \frac{\lambda_j(q) e^{i\vec{q} \cdot \vec{r}}}{1 + u(q)\lambda_j(q)} . \quad (2.7)$$

The ideal-gas term is eliminated, and it is much easier to treat Eq. (2.7) than Eq. (2.1) because the numerator of integrand in the latter is linear in $\lambda_j(q)$.

In terms of the pair distribution function, the internal energy is given by

$$U(T) = U_0(T) + \frac{A}{2} \int_0^1 d\xi \int d\vec{r} \phi(r) \frac{\partial}{\partial \beta} [\beta \rho_2(r, \beta, \xi)] , \quad (2.8)$$

where ξ is a coupling constant, $U_0(T)$ is the ideal-gas energy, A is the two-dimensional volume, and $\phi(r)$ is the two-body interaction potential. Substituting Eq. (2.7) for the pair distribution function into Eq. (2.8), we obtain the internal energy as

$$\begin{aligned} U(T) = U_0(T) + \frac{n^2 A}{2} \int d\vec{r} \phi(r) - \frac{1}{2} nA \int \frac{d\vec{q}}{(2\pi)^2} u(q) \\ + \frac{A}{2} \frac{\partial}{\partial \beta} \left[\sum_{j=-\infty}^{\infty} \int_0^1 d\xi \int \frac{d\vec{q}}{(2\pi)^2} \frac{u(q) \lambda_j(q)}{1 + \xi u(q) \lambda_j(q)} \right] . \end{aligned} \quad (2.9)$$

The effective eigenvalues $\lambda_j(q)$ evaluated to first-order from Eq. (2.3) are given by

$$\lambda_j(q) = \frac{2nq^2}{q^2 + \left(\frac{2\pi j}{\beta}\right)^2} , \quad (2.10)$$

and substitution of Eq. (2.10) into (2.9) yields the final expression for the internal energy at absolute zero temperature as

$$\begin{aligned}
U(T) = & \frac{1}{2} n^2 A \int d\vec{r} \phi(r) + \frac{A}{2} \int \frac{d\vec{q}}{(2\pi)^2} [E(q) - q^2 - nu(q)] \\
& + A \int \frac{d\vec{q}}{(2\pi)^2} E(q) f(E) , \quad (2.11)
\end{aligned}$$

where $f(E) = 1/[e^{\beta E} - 1]$ is the Bose distribution function, and

$$E(q) = [q^4 + 2nu(q)q^2]^{\frac{1}{2}} \quad (2.12)$$

is the excitation energy which was given originally by Bogoliubov and Zubarev.²⁵

In the expression for the internal energy given by Eq. (2.11), the first and second terms represent the ground-state energy and the quasiparticle excitation energy, where the latter demonstrates a Landau-type excitation but does not provide for the temperature variation of the elementary excitation spectrum. For finite temperatures, the above approach is not quite correct; the eigenvalues must have terms which are dependent on the de Broglie thermal wavelength, and we shall discuss this problem in the following sections.

III. Structure factor

In the chain diagram approximation, the structure factor, $S(q)$, is given by the integrand of Eq. (2.7) as

$$S(q) = \frac{1}{\beta n} \sum_j \frac{\lambda_j(q)}{1 + u(q)\lambda_j(q)} \quad (3.1)$$

Combining Eqs. (2.10) and (3.1), we obtain

$$S(q) = \frac{q \coth(\frac{1}{2}\beta q) [q^2 + 2nu(q)]^{\frac{1}{2}}}{[q^2 + 2nu(q)]^{\frac{1}{2}}} \quad (3.2)$$

This result agrees with those obtained by others.²⁶ In order to extend this calculation to higher temperatures, we may use

$$\lambda_j(q) = \lambda_j^0(q) + \Delta\lambda_j(q) \quad , \quad (3.3)$$

where

$$\lambda_j^0(q) = \frac{2nq}{[q^4 + (\frac{2\pi j}{\beta})^2]} - \frac{12n\gamma(z)q^4}{\beta[q^4 + (\frac{2\pi j}{\beta})^2]^2} \quad (3.4)$$

and

$$\Delta\lambda_j(q) = \frac{16\gamma(z)nq^3}{\beta[q^4 + (\frac{2\pi j}{\beta})^2]^3} \quad , \quad \gamma(z) = \frac{G_2(z)}{G_1(z)} \quad , \quad G_s(z) = \sum_{\ell=1}^{\infty} \frac{z^\ell}{\ell^s} \quad (3.5)$$

The structure factor to first order in $\Delta\lambda$ is

$$S(q) = \frac{1}{\beta n} \sum_j \frac{\lambda_j^0(q)}{1 + u(q)\lambda_j^0(q)} + \frac{1}{\beta n} \sum_j \frac{\Delta\lambda_j(q)}{[1 + u(q)\lambda_j^0(q)]^2} \quad (3.6)$$

Substituting Eqs. (3.4)-(3.5) into (3.6) and summing over j , we obtain (see Appendix A)

$$\begin{aligned}
s(q) = & \left\{ \frac{q \coth(\frac{1}{2}\beta q) [q^2 + U_+]^{\frac{1}{2}}}{2[q^2 + U_+]^{\frac{1}{2}}} \left(1 + \frac{2\nu(q) + \alpha}{2[(\nu(q))^2 + \nu(q)d]^{\frac{1}{2}}} \right) \right. \\
& + \frac{q \coth(\frac{1}{2}\beta q) [q^2 + U_-]^{\frac{1}{2}}}{2[q^2 + U_-]^{\frac{1}{2}}} \left(1 - \frac{2\nu(q) + \alpha}{2[(\nu(q))^2 + \nu(q)\alpha]^{\frac{1}{2}}} \right) \Bigg\} \\
& + \left\{ \frac{\alpha q^3 \coth(\frac{1}{2}\beta q) [q^2 + U_-]^{\frac{1}{2}}}{12[(\nu(q))^2 + \nu(q)\alpha]^{\frac{1}{2}} [q^2 + U_-]^{\frac{3}{2}}} \right. \\
& - \frac{\alpha q^3 \coth(\frac{1}{2}\beta q) [q^2 + U_+]^{\frac{1}{2}}}{12[(\nu(q))^2 + \nu(q)\alpha]^{\frac{1}{2}} [q^2 + U_+]^{\frac{3}{2}}} \Bigg\} \\
& + \left\{ \frac{\alpha q^2 (\frac{\beta}{2})^2 \operatorname{csech}^2(\frac{1}{2}\beta q) [q^2 + U_-]^{\frac{1}{2}}}{6\beta[(\nu(q))^2 + \nu(q)\alpha]^{\frac{1}{2}} [q^2 + U_-]^{\frac{1}{2}}} \right. \\
& - \frac{\alpha q^4 \operatorname{csech}^2(\frac{1}{2}\beta q) [q^2 + U_+]^{\frac{1}{2}}}{6\beta[(\nu(q))^2 + \nu(q)\alpha]^{\frac{1}{2}} [q^2 + U_+]^{\frac{1}{2}}} \Bigg\} , \tag{3.7}
\end{aligned}$$

where

$$\alpha(\beta, z) = \frac{12\gamma(z)}{\beta}$$

$$U_+ = \nu(q) \{1 + [1 + \alpha(\beta, z)/\nu(q)]^{\frac{1}{2}}\} \tag{3.8}$$

$$U_- = \nu(q) \{1 - [1 + \alpha(\beta, z)/\nu(q)]^{\frac{1}{2}}\} .$$

In Eq. (3.7), the first bracket represents the first-order modifications, and the second bracket shows the $\Delta\lambda_j$ correction. We will later discuss these terms in detail in Sec. VII.

IV. Elementary excitation spectrum

In Sec. II we used Eq. (2.10), evaluated in the first-order approximation, to obtain the excitation spectrum at absolute zero temperature. In this section we evaluate the temperature variation of the excitation spectrum. Within the chain diagram approximation for the pair distribution function, we have the following expression for internal energy:

$$\begin{aligned}
 U(\beta) = U_0(\beta) + \frac{A}{2} \frac{\partial}{\partial \beta} \left[\beta n^2 \int d\vec{r} \phi(r) - \beta n \int \frac{d\vec{q}}{(2\pi)^2} u(q) \right] \\
 + \frac{A}{2} \frac{\partial}{\partial \beta} \left\{ \sum_j \int \frac{d\vec{q}}{(2\pi)^2} \ln[1 + u(q)\lambda_j(q)] \right\}. \quad (4.1)
 \end{aligned}$$

The above equation for the internal energy is equivalent to the result of the ring diagram. Making use of the first-order approximation for λ_j and summing over j , we arrive at

$$\begin{aligned}
 U(\beta) = U_0(\beta) + \frac{n^2 A}{2} \int d\vec{r} \phi(r) + \beta n n' A \int d\vec{r} \phi(r) \\
 + \frac{A}{2} \int \frac{dq}{(2\pi)^2} \left\{ q^2 \coth\left(\frac{\beta q^2}{2}\right) + nu(q) + \beta n' u(q) \right. \\
 \left. - [q^2 + 2nu(q)]^{\frac{1}{2}} \coth \frac{\beta q^2}{2} \times [q^2 + 2nu(q)]^{\frac{1}{2}} \right\}
 \end{aligned}$$

$$- \frac{\beta n u(q) q \coth(\frac{\beta q^2}{2}) [q^2 + 2n u(q)]^{\frac{1}{2}}}{[q^2 + 2n u(q)]^{\frac{1}{2}}} \} , \quad (4.2)$$

where $n' = [\partial n / \partial \beta]_z$.

The expressions of interest in Eq. (4.2) are the terms that have the form $\frac{1}{2} E(q) \coth[E(q)/2]$, which can be reexpressed as

$$\frac{1}{2} E(q) + E(q) f(E) , \quad (4.3)$$

where $f(E)$ is the Bose distribution function. As can be readily confirmed, the total energy in Eq. (4.2) consists of two parts: one corresponding to the ground-state energy, i.e., the zero-point energy, and the other to quasiparticle excitation energy. Since we are mainly interested in the quasiparticle excitation energy, we will discard the constant ground-state energy term.

Extending this calculation to higher-order in the temperature by including terms of order β^{-1} in the eigenvalues, and using Eq. (3.3) together with Eqs. (3.4) and (3.5) and summing over j , we obtain

$$\begin{aligned} U(\beta) = U_0(\beta) + \frac{n^2 A}{2} \int d\vec{r} \phi(r) + \beta n n' A \int d\vec{r} \phi(r) - \frac{A}{2} \int \frac{d\vec{q}}{(2\pi)^2} n u(q) \\ - \frac{A}{2} \int \frac{d\vec{q}}{(2\pi)^2} \beta n' u(q) + \frac{A}{2} \int \frac{d\vec{q}}{(2\pi)^2} \left\{ \frac{n u(q)}{[(n u(q))^2 + n u(q) \alpha]^{\frac{1}{2}}} q [q^2 + U_+]^{\frac{1}{2}} \right. \\ \left. \times \coth(\frac{\beta q^2}{2}) [q^2 + U_+]^{\frac{1}{2}} - \frac{n u(q) q^2 \alpha \coth(\frac{1}{2} \beta q^2)}{[(n u(q))^2 + n u(q) \alpha]^{\frac{1}{2}} U_+} \right\} \end{aligned}$$

$$\begin{aligned}
& + \frac{nu(q)\alpha}{[(nu(q))^2 + nu(q)\alpha]^{\frac{1}{2}}} \frac{\coth(\frac{\beta q}{2})[q^2 + U_+]^{\frac{1}{2}}}{[q^2 + U_+]^{\frac{1}{2}}} \\
& + \frac{nu(q)\alpha q^3}{[(nu(q))^2 + nu(q)\alpha]^{\frac{1}{2}} U_+} \frac{\coth(\frac{\beta q}{2})[q^2 + U_+]^{\frac{1}{2}}}{[q^2 + U_+]^{\frac{1}{2}}} \\
& + \frac{\beta q \coth(\frac{\beta q}{2})[q^2 + U_+]^{\frac{1}{2}}}{2[q^2 + U_+]^{\frac{1}{2}}} \left\{ n'u(q) + \frac{2nn'u(q)^2 + n'u(q)\alpha + nu(q)\alpha'}{2[(nu(q))^2 + nu(q)\alpha]^{\frac{1}{2}}} \right\} \\
& + \frac{A}{2} \int \frac{d\vec{q}}{(2\pi)^2} \left\{ - \frac{nu(q)q[q^2 + U_-]^{\frac{1}{2}}}{[(nu(q))^2 + nu(q)\alpha]^{\frac{1}{2}}} \coth(\frac{\beta q}{2})[q^2 + U_-]^{\frac{1}{2}} \right. \\
& + \frac{nu(q)\alpha q^2 \coth(\frac{1}{2} \beta q^2)}{[(nu(q))^2 + nu(q)\alpha]^{\frac{1}{2}} U_-} - \frac{nu(q)\alpha q}{[(nu(q))^2 + nu(q)\alpha]^{\frac{1}{2}}} \\
& \times \frac{\coth(\frac{\beta q}{2})[q^2 + U_-]^{\frac{1}{2}}}{[q^2 + U_-]^{\frac{1}{2}}} - \frac{nu(q)\alpha q^3}{[(nu(q))^2 + nu(q)\alpha]^{\frac{1}{2}} U_-} \frac{\coth(\frac{\beta q}{2})[q^2 + U_-]^{\frac{1}{2}}}{[q^2 + U_-]^{\frac{1}{2}}} \\
& \left. + \frac{\beta q \coth(\frac{\beta q}{2})[q^2 + U_-]^{\frac{1}{2}}}{2[q^2 + U_-]^{\frac{1}{2}}} \left\{ n'u(q) - \frac{2nn'u(q)^2 + n'u(q)\alpha + nu(q)\alpha'}{2[n^2u(q)^2 + nu(q)\alpha]^{\frac{1}{2}}} \right\} \right\} ,
\end{aligned}
\tag{4.4}$$

where $\alpha' = (\partial\alpha/\partial\beta)_Z$. As we did before, taking only the quasiparticle excitation spectrum from Eq. (4.4), we get

$$E(T) = \left\{ \frac{nu(q)q[q^2 + U_+]^{\frac{1}{2}}}{[(nu(q))^2 + nu(q)\alpha]^{\frac{1}{2}}} - \frac{nu(q)\alpha q^2}{[(nu(q))^2 + nu(q)\alpha]^{\frac{1}{2}} U_+} \right.$$

$$\begin{aligned}
& + \frac{nu(q)\alpha q}{[(nu(q))^2 + nu(q)\alpha]^{\frac{1}{2}}[q^2 + U_+]^{\frac{1}{2}}} + \frac{nu(q)\alpha q^3}{[(nu(q))^2 + nu(q)\alpha]^{\frac{1}{2}}[q^2 + U_+]^{\frac{1}{2}}U_+} \\
& + \frac{\beta q}{2[q^2 + U_+]^{\frac{1}{2}}} \left\{ nn' + \frac{2nn'u(q)^2 + n'u(q)\alpha + nu(q)\alpha'}{2[(nu(q))^2 + nu(q)\alpha]^{\frac{1}{2}}} \right\} \\
& + \left\{ - \frac{nu(q)q[q^2 + U_-]^{\frac{1}{2}}}{[(nu(q))^2 + nu(q)\alpha]^{\frac{1}{2}}} + \frac{nu(q)\alpha q^2}{[(nu(q))^2 + nu(q)\alpha]^{\frac{1}{2}}U_-} \right. \\
& - \frac{nu(q)\alpha q}{[(nu(q))^2 + nu(q)\alpha]^{\frac{1}{2}}[q^2 + U_-]^{\frac{1}{2}}} - \frac{nu(q)\alpha q^3}{[(nu(q))^2 + nu(q)\alpha]^{\frac{1}{2}}[q^2 + U_-]^{\frac{1}{2}}U_-} \\
& \left. + \frac{\beta q}{2[q^2 + U_-]^{\frac{1}{2}}} \left\{ nn' - \frac{2nn'u(q)^2 + n'u(q)\alpha + nu(q)\alpha'}{2[(nu(q))^2 + nu(q)\alpha]^{\frac{1}{2}}} \right\} \right\} . \quad (4.5)
\end{aligned}$$

In Eq. (4.5), the terms inside the first bracket represent the temperature-dependent phonon spectrum, while the second bracket corresponds to the free particle in nature. Equation (4.5) reduces to the excitation spectrum [Eq. (2.12)] at absolute zero temperature because $\alpha(\beta, z)$ tends to zero in this limit. Since α depends on Bose statistics, the excitation spectrum depends on statistics.

To have a more explicit form for the excitation spectrum, we may choose a mock potential. However, we have adopted a soft potential with a Lennard-Jones-type tail in our previous works, which we introduce again here, i.e.,

$$\phi(r) = \begin{cases} V_0, & r \leq a \\ E_0 \left[\left(\frac{a}{r} \right)^{12} - \left(\frac{a}{r} \right)^6 \right], & r \geq a \end{cases} \quad (4.6)$$

From the Fourier transform of this soft potential, we may find an expression¹³ for small q ,

$$2\nu(q) = A^2(0) + A_1^2 q^2 + A_2^2 q^4 - A_3 q^4 \ln(qa) - A_4 q^6 + \dots, \quad (4.7)$$

where the coefficients A_i are given as

$$A^2(0) = 2\pi n a^2 (V_o - \frac{3}{10} E_o), \quad A_1^2 = \frac{\pi n a^4}{2} (\frac{3}{2} E_o - V_o), \quad (4.8)$$

$$A_2^2 = 4\pi n a^6 \left\{ \frac{V_o}{2^6 \times 3!} - \frac{E_o}{10 \times 10!!} (1016 + 48 \times 10^2 \gamma) \right\}; \quad \gamma = 0.5771.$$

For small q and the low-temperature region, substituting Eq. (4.7) into Eq. (4.5), the temperature variation of the phonon spectrum can be evaluated from the expansion

$$E(q, T) = (A_o + \frac{\alpha}{4A_o}) q - \frac{\alpha}{A_o^2} q^2 + [B - \frac{\alpha}{8A_o^3} (A_1^2 + 1)] q^3 + \frac{\alpha A_1^2}{A_o^4} q^4 + \left[C - \frac{3\alpha}{8A_o^3} \left(\frac{A_2^2}{3} - \frac{A_1^4}{4A_o^2} - \frac{A_1^2}{2A_o^2} \right) \right] q^5 + \dots, \quad (4.9)$$

where

$$B = (1 + A_1^2)/2A_o, \quad C = \frac{1}{2A_o} \left[A_2^2 - \frac{(1 + A_1^2)^2}{4A_o} \right].$$

We can easily confirm that Eq. (4.9) is the elementary excitation spectrum of the Bose liquid at very low momenta, and as $T \rightarrow 0$, α tends to zero, so that Eq. (4.9) reduces to what we have derived for the spectrum at absolute zero temperature,¹⁴

$$E(q) = A(0)q + Bq^3 + Cq^5 + \dots \quad (4.10)$$

For large q , we take only the dominant term to get

$$E(q) = q[q^2 + (4\pi na^2/qa)V_0 J_1(qa)]^{1/2} \quad (4.11)$$

The Bessel function J_1 is oscillatory, and hence there can be a minimum in the energy curve. Around this minimum one can find the familiar roton spectrum¹

$$E(q) = \Delta + \frac{\hbar^2}{2m^*} (q - q_0)^2, \quad (4.12)$$

where m^* , Δ and q_0 are the roton effective mass, energy gap and minimum point, respectively.

V. Thermodynamic functions

In the view of the energy spectrum, we follow Landau's theory to obtain the phonon and roton energies. Using the small and large q expansions of the energies, i.e., Eqs. (4.9) and (4.12), we obtain the thermodynamic functions in a straightforward fashion as

$$E_{ph}(T) = \frac{1}{2\pi} \left\{ \frac{2\zeta(3)}{A^2(0)} (k_B T)^3 + \frac{2 \cdot 3! \gamma(2) \zeta(3)}{A^4(0)} (k_B T)^4 \right.$$

$$= \frac{4 \cdot 4! \zeta(5) B}{A^5(0)} \left[1 + \frac{3 \zeta(4) \gamma(Z)}{4 \zeta(5) B} \right] (k_B T)^5 + \frac{6! \zeta(7) C}{A^7(0)} (k_B T)^7 + \dots \quad (5.1)$$

$$E_{\text{rot}}(T) = \left(\frac{m^* k_B T}{2\pi \hbar^2} \right)^{3/2} q_0 \left[\Delta + \frac{1}{2} (k_B T)^2 \right] e^{-\Delta/k_B T} \quad (5.2)$$

The corresponding specific heats are given by

$$C_{V_{\text{ph}}}(T) = \frac{k_B}{2\pi} \left\{ \frac{3! \zeta(3)}{A^2(0)} (k_B T)^2 + \frac{2 \cdot 4! \gamma(Z) \zeta(3)}{A^4(0)} (k_B T)^3 \right. \\ \left. - \frac{4 \cdot 5! \zeta(5) B}{A^5(0)} \left[1 + \frac{3 \zeta(4) \gamma(Z)}{4 \zeta(5) B} \right] (k_B T)^4 + \frac{7! \zeta(7) C}{A^7(0)} (k_B T)^6 + \dots \right\} \quad (5.3)$$

$$C_{V_{\text{rot}}}(T) = \left(\frac{m^* k_B T}{2\pi \hbar^2} \right)^{3/2} k_B q_0 \left[\frac{3}{4} + \frac{\Delta}{k_B T} + \left(\frac{\Delta}{k_B T} \right)^2 \right] e^{-\Delta/k_B T} \quad (5.4)$$

The theoretical expressions for other thermodynamical functions are

$$F_{\text{ph}}(T) = - \frac{1}{2\pi} \left\{ \frac{\zeta(3)}{A^2(0)} (k_B T)^3 - \frac{6 \gamma(Z) \zeta(3)}{A^4(0)} (k_B T)^4 \right. \\ \left. - \frac{4! \zeta(5) B}{A^5(0)} \left[1 - \frac{3 \gamma(Z) \zeta(4)}{A(0) B \zeta(5)} \right] (k_B T)^5 - \frac{6! \gamma B \zeta(5)}{A^6(0)} (k_B T)^6 + \dots \right\} \quad (5.5)$$

$$F_{\text{rot}}(T) = - q_0 \left(\frac{m^*}{2\pi \hbar^2} \right)^{3/2} (k_B T)^{3/2} e^{-\Delta/k_B T} \quad (5.6)$$

$$S_{\text{ph}}(T) = \frac{k_B}{2\pi} \left\{ \frac{3 \zeta(3)}{A^2(0)} (k_B T)^2 - \frac{4! \gamma(Z) \zeta(3)}{A^4(0)} (k_B T)^3 \right.$$

$$\begin{aligned}
& - \frac{5\zeta(5)B}{A^5(0)} \left[1 - \frac{3\gamma(z)\zeta(4)}{BA(0)\zeta(5)} \right] (k_B T)^4 - \frac{180 \cdot 3! \gamma(z) B \zeta(5)}{A^6(0)} (k_B T)^5 \\
& + \frac{105 \cdot 5! \zeta(7)}{A^7(0)} (k_B T)^6 + \dots \} , \quad (5.7)
\end{aligned}$$

$$S_{\text{rot}}(T) = \left(\frac{m^* k_B T}{2\pi \hbar^2} \right)^{3/2} k_B q_0 \left[\frac{3}{2} + \frac{\Delta}{k_B T} \right] e^{-\Delta/k_B T} , \quad (5.8)$$

$$\begin{aligned}
P_{\text{ph}}(T) &= \frac{1}{\pi} \left\{ \frac{\zeta(3)}{A^2(0)} (k_B T)^3 - \frac{9\gamma(z)\zeta(3)}{A^4(0)} (k_B T)^4 \right. \\
&\quad \left. - \frac{2 \cdot 4! \zeta(5) B_1}{A^5(0)} \left[1 - \frac{3 \cdot \gamma(z) \zeta(4)}{A(0) B_1 \zeta(5)} \right] (k_B T)^5 + \dots \right\} , \quad (5.9)
\end{aligned}$$

$$P_{\text{rot}}(T) = \left(\frac{m^*}{2\pi \hbar^2} \right)^{3/2} q_0 (k_B T)^{3/2} e^{-\Delta/k_B T} . \quad (5.10)$$

If the quasiparticles move with an average drift velocity with respect to the rest system, and this momentum is associated with the normal fluid, then its density is given by

$$\rho_N(T) = - \frac{1}{4\pi} \int_0^\infty q^3 dq \left\{ \frac{\partial f(E(q))}{\partial E(q)} \right\} . \quad (5.11)$$

Since the normal fluid consists of the phonon and roton parts, from Eq. (5.11) we can obtain directly

$$\begin{aligned}
\rho_N(T) &= \frac{3! \zeta(3) \hbar}{4\pi A(0)} \left(1 - \frac{\alpha}{4A(0)} \right) \left(\frac{k_B T}{\hbar A(0)} \right)^3 + \frac{6 \cdot 3! \zeta(4) \alpha \hbar}{A^4(0)} \left(\frac{k_B T}{\hbar A(0)} \right)^4 + \dots , \\
&\quad (5.13)
\end{aligned}$$

$$\rho_{\text{rot}}(T) = \frac{1}{2} \left(\frac{m^* \hbar^2}{2\pi k_B T} \right)^{3/2} q_0^3 e^{-\Delta/k_B T} \quad (5.14)$$

We note that Eqs. (5.1)-(5.14) are reduced to the thermodynamic functions in Ref. 8 when we take α to be zero.

VI. First, second and third sound

For temperatures below 0.6 K where the roton excitation can be neglected, there has been confusion regarding the normal and anomalous excitation spectrums. Some researchers^{27,28} have used the wrong normal dispersion to obtain the temperature variation of the first sound. Maris and Massey²⁹ pointed out that the dispersion relation should be anomalous due to ultrasonic attenuation.

As we mentioned earlier, we have derived the anomalous excitation spectrums and introduced a new approach^{15,16} which includes a collision term in the Boltzmann equation, and obtained the first and second sound simultaneously. At low frequencies such that $\omega_s \tau \ll 1$, where ω_s is the sound frequency and τ is the characteristic time, one can make use of a hydrodynamical approach to sound propagation, and for the opposite case of $\omega_s \tau \gg 1$, it is appropriate to make use of the kinetic equations. We shall evaluate the first and second sounds in the kinetic approach. Since we have treated the kinetic approach in detail,¹⁶ we will briefly review only the essential features and give the results on the basis of our new temperature-dependent excitation spectrums.

We solve the equation of motion for the velocities of first and second sound for temperatures below 0.6 K where roton excitation is negligible but phonon excitation dominates. Our approach is similar to that developed by

Andreev and Khalatnikov²⁷ and Disatnik,³⁰ and in order to obtain both the first and second sounds, we include a collision term and treat the kinetic equation for the phonon distribution function $n(\vec{p}, \vec{r}, t)$, equation of continuity, and equation for the superfluid velocity \vec{v}_s . When the liquid is slightly perturbed from equilibrium, we assume that the perturbation terms from the distribution mass density ρ and superfluid velocity (\vec{v}_s) are proportional to $\exp[i(\vec{k} \cdot \vec{r} - \omega_s t)]$. Here \vec{k} is the complex wave vector $\vec{k}_1 + i\vec{k}_2$, where the ratio k_2/k_1 characterizes the attenuation of sound. When $k_2/k_1 \ll 1$, we may linearize the above mentioned three perturbed terms for n' , ρ' and v'_s . To simplify, we adopt the single collision model and use our excitation spectrum, obtaining two linear homogeneous equations in ρ'/ρ and v'_s/c :

$$\begin{aligned} & \left[\left\{ 1 + \frac{1}{i\omega\tau} \right\} - \frac{1}{i\omega\tau} \left\{ 1 - 2u \frac{C_o}{C} \frac{\omega_s}{kC} \xi_T \right\} g(\xi_T) - 2 \left\{ u \frac{C_o}{C} \right\}^2 \frac{\rho_n}{\rho_o} g(\xi_T) \right] \frac{\rho'}{\rho_o} \\ & - \left[\left\{ 1 + \frac{1}{i\omega\tau} \right\} \frac{\omega_s}{kC} - \frac{1}{i\omega\tau} \left\{ \frac{\omega_s}{kC} - 2u \frac{C_o}{C} \xi_T \right\} g(\xi_T) + 2u \frac{C_o}{C} \frac{\rho_n}{\rho_o} \xi_T g(\xi_T) \right] \frac{v'_s}{C} = 0, \end{aligned} \quad (6.1)$$

$$\begin{aligned} & \left[u \frac{C_o}{C} \frac{\omega_s}{kC} + \frac{1}{i\omega\tau} \left\{ 1 - 2u \frac{C_o}{C} \frac{\omega_s}{kC} \xi_T \right\} g(\xi_T) + 2 \left\{ u \frac{C_o}{C} \right\}^2 \frac{\rho_n}{\rho_o} \xi_T g(\xi_T) \right] \frac{\rho'}{\rho} \\ & - \left[u \frac{C_o}{C} + \frac{1}{i\omega\tau} \xi_T \left\{ \frac{\omega_s}{kC} - 2u \frac{C_o}{C} \xi_T \right\} g(\xi_T) - 2u \frac{C_o}{C} \frac{\rho_n}{\rho_o} \left[\frac{1}{2} + \xi_T^2 g(\xi_T) \right] \right] \frac{v'_s}{C} = 0, \end{aligned} \quad (6.2)$$

where

$$\xi_T = \frac{\omega}{kv(T)} \quad , \quad g(\xi_T) = 1 - \frac{\omega/kv(T)}{[(\omega/kv(T))^2 - 1]^{1/2}} \quad (6.3)$$

A nontrivial solution can be obtained from Eqs. (6.1) and (6.9) under the condition that

$$\begin{aligned} \left[\left(\frac{\omega_s}{kC} \right)^2 - 1 + \frac{\rho_n}{\rho_o} \right] \phi - 2 \frac{\rho_n}{\rho_o} \left(\frac{C_o}{C} \right)^2 \left[\left[u^2 + \frac{C^2}{C_o v(T)} \left(\frac{\omega_s}{kC} \right)^2 \right] \right. \\ \left. \times \left\{ 2u + \frac{C^2}{C_o v(T)} \right\} \right] - 2u^2 \left(\frac{C_o}{C} \right)^2 \left(\frac{\rho_n}{\rho_o} \right)^2 = 0 \end{aligned} \quad (6.4)$$

where we replace the group velocity by its thermal average to obtain

$$v(T) = C_o (1 + \alpha' + 3\gamma' P_T^2 + \dots) \quad , \quad (6.5)$$

$$\alpha' = \frac{12\gamma(z)}{4A^2(0)} (1 - \frac{2}{A(0)} q) k_B T \quad , \quad \gamma' = \frac{\gamma}{\hbar^2} \quad , \quad (6.6)$$

and

$$\phi = \frac{1 - i\omega_s \tau g(\xi_T)^{-1}}{i\omega_s \tau - 1} + \frac{2\xi_T^2}{i\omega_s \tau} \quad (6.7)$$

Since the expression C can be written as

$$C^2 = C_o^2 + \frac{2}{3} C_o \rho_o^2 \frac{\rho_n}{\rho_o} \frac{\partial^2 C_o}{\partial \rho_o^2} \approx C_T^2 + 2u^2 C_o^2 \frac{\rho_n}{\rho_o} \quad , \quad (6.8)$$

where $C_T^2 = (\partial P / \partial \rho)_T$ is the isothermal sound velocity, we find the unknown in Eq. (6.4) to be ω_s / kC_0 or ω_s / kC_T . From Eq. (6.4) we can obtain the solutions for the hydrodynamical region ($\omega_s r \ll 1$) and collisionless region ($\omega_s r \gg 1$).

A. Hydrodynamic region ($\omega_s r \ll 1$)

In the low frequency limit ($\omega_s r \ll 1$), ϕ can be approximated as

$$\phi \approx -1 + 2\xi_T^2 - \frac{1}{2}[\xi_T^2 - 1]i\omega_s r \quad (6.9)$$

Substitution of Eq (6.9) into (6.4) yields a quadratic equation in $(\omega_s / kC)^2$. Solving Eq. (6.4) for $(\omega_s / kC)^2$ together with Eq. (6.8), we obtain the first and second sounds and their attenuation coefficients:

$$\frac{C_1(T)}{C_T} = 1 + \frac{\rho_n}{\rho_0} \left\{ (2u+1)^2 + 2(2u^2+3u+1)\alpha + (6u^2+5u+1)\beta \right\} \quad (6.10)$$

$$\left(\frac{k_2}{k_1} \right)_1 = \frac{\omega_s r}{8} \left\{ \frac{\rho_n}{\rho_0} (2u^2+3u+1) - \frac{1}{4}(2\alpha+\beta) \right\} \quad (6.11)$$

$$\frac{C_2(T)}{C_T} = \frac{1}{\sqrt{2}} \left\{ 1 + \frac{1}{2}(2\alpha+\beta) - \frac{\rho_n}{\rho_0} (u+1)^2 \right\} \quad (6.12)$$

$$\left(\frac{k_2}{k_1} \right)_2 = \frac{\omega_s r}{8} \left[1 + (7u^2+4u+1) \frac{\rho_n}{\rho_0} \right] \quad (6.13)$$

where α and β are given by

$$\alpha = \alpha' + 3\gamma P_T^2 - 5\delta P_T^4, \quad \beta = -\frac{2}{3} \left(\frac{\rho_0^2}{C_0} \right) \left(\frac{\partial^2 C_0}{\partial \rho^2} \right) \frac{\rho_n}{\rho_0} \quad (6.14)$$

with

$$\delta = [2A^2(0)]^{-1} [A_2^2 - (1+A_1^2)^2/4A^2(0)] .$$

B. Collisionless region ($\omega_s \tau \gg 1$)

In the high-frequency limit, we can approximate Eq. (6.7) as

$$\phi = -\frac{3}{2}(1-\alpha) + 2\xi_T^2 - \frac{(1-\alpha)}{2i\omega_s \tau} . \quad (6.15)$$

Substituting Eq. (6.15) into (6.4) and solving the quadratic Eq. (6.4) for $(\omega_s/kC)^2$, we obtain the velocities of the first and second sounds and corresponding attenuation coefficients:

$$\frac{C_1(T)}{C_T} = 1 + \frac{1}{2}[(6u^2+8u+3) + (8u^2+15u+6)\alpha + (10u^2+11u+3)\beta] , \quad (6.16)$$

$$\left(\frac{k_2}{k_1}\right)_1 = \frac{1}{2\omega_s \tau} \left[\frac{1}{8}(6\alpha+3\beta) + (u+1)\frac{\rho_n}{\rho_o} \right] , \quad (6.17)$$

$$\frac{C_2(T)}{C_T} = \frac{\sqrt{3}}{2} \left[1 + (\alpha' + 3\gamma P_T^2 - 5\delta P_T^4) - \frac{1}{3} \left\{ (5u^2+12u+6) + \frac{\rho_o^2}{C_o} \frac{\partial^2 C_o}{\partial \rho^2} \right\} \frac{\rho_n}{\rho_o} \right] , \quad (6.18)$$

$$\left(\frac{k_2}{k_1}\right)_2 = \frac{1}{6\omega_s \tau} \left[1 - 2(\alpha' + 3\gamma P_T^2 - 5\delta P_T^4) + \frac{1}{3} \left\{ 11u^2 - 6 + 2 \frac{\rho_o^2}{C_o} \frac{\partial^2 C_o}{\partial \rho^2} \right\} \frac{\rho_n}{\rho_o} \right] . \quad (6.19)$$

In the derivation of Eq. (6.4), we have adopted the single-collision time model for the collision integral term. If we neglect these collisions among excitations and solve this equation for (ω_s/k) , we obtain

$$\delta C = \frac{\omega_s}{k} - C_0 = -C_0 \left[(u+1)^2 + \frac{1}{2} - \frac{1}{3} \frac{\rho_0^2}{C_0} \frac{\partial^2 C_0}{\partial \rho^2} - 2(u+1)^2 \alpha \right] \frac{\rho_n}{\rho_0} \quad (6.20)$$

We note that except for the α term, Eq. (6.20) is identical to what we have derived in our previous paper.¹⁵

In the case of low frequencies ($\omega_s \tau \ll 1$), we can apply the superfluid hydrodynamics equations together with the dissipation function to obtain the first and second sounds. However, this derivation is not related directly to our new temperature variation of the excitation spectrum, and thus we will not discuss this here.

Since the third sound in superfluid helium films has been observed in both thick and thin films,³¹ researchers³² have investigated this sound in different ways. Recently we have also analyzed thin film data in terms of the elementary excitations obtained by a microscopic approach.¹⁷ Using these previous results and the new temperature-dependent excitation spectrum, we will reanalyze the third sound data.

When sound waves with wavelength longer than the film thickness propagate along a helium film, the normal fluid is held rigid to the substrate, while the superfluid shows density fluctuations. For the third sound velocity, we make use of the formula

$$C_3^2(T) = \frac{1}{m} \rho_s(T) \kappa(T) \quad , \quad (6.21)$$

where m is the helium mass, $\rho_s(T)$ is the superfluid number density, and the adiabatic elastic constant κ can be obtained from the second derivative of the excitation spectrum with respect to the surface number density n . Using Eqs. (5.1), (5.13) and (5.14), we obtain the third sound velocity

$$C_3^2(T) = C_0^2 [1 + X_1 (k_B T)^3 + X_2 (k_B T)^4 + X_3 (k_B T)^5 + X_4 (k_B T)^{-1/2} e^{-\Delta/k_B T} + X_5 (k_B T)^{5/2} e^{-\Delta/k_B T} + \dots] , \quad (6.22)$$

where

$$\begin{aligned} V_o^* &= V_o - \frac{3}{10} E_o , \\ D_1 &= (2\pi a^2 V_o^*)^{1/2} \\ D_2 &= \frac{1}{4} \pi a^4 \left(\frac{3}{2} E_o - V_o \right) , \\ B &= \pi a^2 V_o^* \left[1 + \frac{a^2}{16} V_o^* (3 + 2 \ln(n a^4 V_o^*)) \right] , \end{aligned} \quad (6.23)$$

and the coefficients C_o and X_i are given by

$$\begin{aligned} C_o^2 &= \frac{nB}{m^*} , \\ X_1 &= \frac{\zeta(3)}{\pi D_1^2 n^3} \left[\frac{2}{B} \left(1 - \frac{3\alpha}{2D_1^2 n} \right) - \frac{3}{D_1^2} \left(1 - \frac{\alpha}{D_1^2 n} \right) \right] \\ X_2 &= \frac{3! \alpha \zeta(4)}{\pi n^5 D_1^6} \left(\frac{18}{B} - \frac{10}{D_1^2} \right) , \\ X_3 &= - \frac{4! \zeta(5)}{\pi n^5 D_1^6} \left[\frac{2}{B} \left(6 + 3nD_2 - \frac{10\alpha}{nD_1^2} - \frac{6\alpha D_2}{D_1^2} \right) - \frac{15}{2D_1^2} (1 + nD_2) \left(1 - \frac{2\alpha}{nD_1^2} \right) \right] , \end{aligned} \quad (6.24)$$

$$X_4 = - \frac{q_0^3}{n} \left(\frac{m^*}{2\pi} \right)^{1/2} ,$$

$$X_5 = - \frac{2\zeta(3)q_0^3}{\pi n^4 B D_1^2} \left(1 - \frac{3\alpha}{2nD_1^2} \right) \left(\frac{m^*}{2\pi} \right)^{1/2} .$$

As in Eq. (4.12), m^* , Δ and q_0 are the roton effective mass, energy gap and minimum point, respectively. These parameters are given as a function of the potential parameters in our previous work.¹³ In Eq. (6.22) the first term is associated with the ground-state energy, and the next three and remaining exponential potential terms are related to the phonon and roton energies, respectively.

VII. Results and discussion

In the previous sections we introduced the eigenvalues of the effective boson propagator and the effective eigenvalue for higher temperatures, and then we evaluated the temperature-dependent structure factor and elementary excitation spectrum. We used these quantities to obtain thermodynamic functions, fluid density and various sounds in thin liquid ^4He films.

The elementary excitation spectrum can generally be determined from neutron scattering measurements³³ and various sound velocity data.³⁴ However, the shape of the spectrum in the very low-momentum region can not be determined well by such experimental methods, but it can be done indirectly from specific heat measurements. The existence of the anomalous phonon spectrum (concave up) was revealed in the first measurements of the specific heat above 0.3 K by Phillips et al.³⁵ More recently, Greywall³⁶ has measured the specific heat of bulk liquid helium with high precision in the temperature

range from 65 to 80 mK and for various molar volumes under high pressure up to 25 bars. The analysis of these data³⁷ through our excitation spectrum at absolute zero temperature gives the anomalous phonon dispersion and also agrees with the results obtained by sound propagation.

Concerning the specific heat of thin liquid ^4He monolayer films, there are several measurements of the heat capacity of ^4He films adsorbed on various substrates.³⁸ Among these, we now analyze the specific data of ^4He monolayers adsorbed on "Grafoil graphite" substrates³⁹ by using our Eqs. (5.3) and (5.4) at $\gamma(Z) = 0$. Here, we assume that: (1) the interaction between ^4He atoms is a soft potential, (2) the system is perfectly two dimensional, and (3) substrate effects are negligible.

Concerning substrate effects, Krotscheck⁴⁰ considered that the liquid helium is translationally invariant in the xy-plane, using three z-dependent substrate potentials $U(z)$, i.e., the Aziz potential,⁴¹ artificially-weakened Aziz potential and Dupont-Roc potential,⁴² which model the adhesion force between the ^4He atom and substrate. He then displayed the one-body densities $\rho(z)$ for the above three potential models for helium films of the different surface coverages and made use of them to evaluate the correlation energy and collective excitation energy. Adopting Krotscheck's method, the number density, which we should treat, will be changed. Then, in order to fit the specific heat data, another sets of parameters in Table I should be chosen. However, in the analysis of the superfluid properties of the helium films, we proved that L/D_0 ,⁴³ where L is the healing length and D_0 is one statistical atomic layer ($D_0 = 3.6\text{\AA}$), by one standard layer thickness is almost constant below 1 K. Therefore, to simplify the problem we have neglected the substrate effect.

When the phonon part is truncated after the third term, we obtain the numerical values for the parameters that give the best results for fitting the specific heat data at various densities, which are listed in Table I. When higher-order terms of the phonon part are included, another set of parameters should be found.

Figure 1 illustrates our theoretical specific heat in comparison with experimental data. At temperatures between 0.5 and 0.6 K, the phonon and roton contributions are comparable for the given densities, and the latter becomes dominant as the temperature increases. In the range of temperatures around 1.2 ~ 1.6 K, the phonon part increases but the roton part decreases more rapidly and hence dominates the overall behavior. Thus the specific heat reaches a maximum, which depends on the density, and then falls sharply. When we determine the temperature T_λ at which the density becomes equal to the actual density of liquid ^4He , we find $T_\lambda = 1.5$ K at the density of $2.79 \times 10^{-2} \text{ \AA}^{-2}$. Adjusting this value in accordance with the ratio of the theoretical and experimental values for bulk ^4He , we obtain $T_\lambda = 1.2$ K. Bishop and Reppy⁴⁴ measured the superfluid transition temperature of a thin helium film adsorbed on an oscillating substrate and reported $T_\lambda = 1.215$ K, which is in excellent agreement with our estimate. In Eq. (5.3) the specific heat varies as T^2 at very low temperatures when $\gamma(Z)$ is zero. This variation is an essential characteristic of a two-dimensional continuum and two-dimensional Debye model.

Figures 2 and 3 represent the elementary excitation spectrums and structure factors, respectively, deduced from the numerical values of the parameters at various densities in Table I. Because of the scale factor, the upward dispersion is not shown clearly in Fig. 2, but we have previously reported that the upward bending becomes stronger as the density increases in two dimensions.^{17,43} In Fig. 2, as the density increases the sound velocity

and roton energy gap increase, but for the case of structure factors we can not find a general tendency as for the excitation spectrums.

Let us now return to the temperature variation of the structure factors. In Eq. (3.7) the first bracket expresses the first-order modification due to the finite temperature. The effect of this finite temperature comes from the effective interaction $U_{\pm}(q, \beta, z)$. The second bracket represents the $\Delta\lambda_j(q)$ correction terms. For low temperatures and small q at fixed density, the interaction effect of $U_{\pm}(z, \beta, z)$ appears since $\alpha(\beta, z)$ has finite growing values with increasing temperature. Therefore, Eq. (3.7) gradually has larger fixed values as $q \rightarrow 0$. We can easily confirm that in the limit $T \rightarrow 0$ and $\alpha(\beta) \rightarrow 0$, Eq. (3.7) is reduced to the zero-temperature expression of Eq. (3.1). We note that $\alpha(\beta, z)$ depends on statistics because of the factor $\gamma(z)$.

To draw the structure factor and excitation spectrum, we must first evaluate $\gamma(z)$ as a function of temperature. However, $\gamma(z)$ can not be represented as a finite closed function (see Appendix B), and so we evaluate these values numerically as a function of temperature.⁴⁵ Figure 4 illustrates $\gamma(z)$ versus temperature, and the results of the numerical calculations for $\gamma(z)$ are listed in Table II.

In order to fit the specific heat data at the density of $2.79 \times 10^{-2} \text{ \AA}^{-2}$, using Eqs. (5.3) and (5.4) which include the $\gamma(z)$ term, we have chosen the potential and roton parameters as

$$\begin{aligned} a &= 3.95 \text{ \AA} , & V &= 8.75 \text{ K} , & E_0 &= 7.49 \text{ K} , & q_0 &= 0.814 \pm 0.302 , \\ m^* &= 2.04 m , & \Delta &= 3.35 \text{ K} . \end{aligned}$$

Figure 5 illustrates the elementary excitations as a function of temperature using the above parameters. As the temperature increases, the phonon part

shows strong upward bending. However, the roton energy gap decreases significantly with increasing temperature, while the roton momentum q_0 maintains almost the same values and thus seems to be independent of temperature.

Figure 6 represents the theoretical temperature dependence of the structure factor. This factor takes on gradually larger values with increasing temperature as $q \rightarrow 0$. The peak becomes higher for higher temperatures because the roton energy gap decreases with increasing temperature. This result agrees with the temperature dependence of the liquid structure function obtained in a variational density matrix approach for liquid ^4He at nonzero temperatures.⁴⁶ Extending Landau's theory, Bendt, Cowan and Yarnell⁴⁷ took into account the temperature dependence of the excitation energy curve in the temperature range 1.1 - 1.8 K, showing that the excitation spectrum generally decreases with increasing temperatures. Recently Suebka and Lu⁴⁸ adopted a modified Brueckner-Sawada method⁴⁹ together with an external potential and reproduced the results given by Bendt et al.

Campbell et al.⁵⁰ employed a variational density matrix theory, together with the minimum principle of the Helmholtz free energy, to derive the elementary excitation spectrum and the structure factor. Their results agreed very well with the experimentally-determined energy of Cowley and Wood⁵¹ at low momentum ($k \leq 0.4 \text{ \AA}^{-1}$), and their excitation spectrum exhibits strong anomalous dispersions with increasing temperature at very short wavelengths. We note that Isihara and Samulski⁵ showed that within the chain diagram approximation the excitation spectrum decreases, while the structure factor increases with temperature in bulk liquid ^4He .

We note that for the thermodynamic functions the phonon part contains both odd and even functions of temperature, and for the specific heat the

leading term is quadratic in temperature, which is characteristic of two dimensions. The roton part is characterized by the energy gap Δ and roton momentum q_0 . Because of the exponential factor, it is small for low temperatures.

In Sec. VI we adopted the single-collision time method model for the collision term and obtained the first and second sounds. Making use of Eq. (6.8), we can express Eqs. (6.10) and (6.16) as follows:

$$\delta C_1(T) = C_1(T) - C_0$$

$$= \frac{C_0 \rho_n}{\rho_0} \left\{ (u+1)^2 - \frac{1}{2} + \frac{1}{3} \frac{\rho_0^2}{C_0} \frac{\partial^2 C_0}{\partial \rho_0^2} + (u+1)(2u+1)\alpha + \frac{1}{2}(3u+1)(2u+1)\beta \right\} ,$$

$$\omega_s \tau \ll 1 , \quad (7.1)$$

$$\delta C(T) = \frac{C_0 \rho_n}{\rho_0} \left\{ 2(u+1)^2 - \frac{1}{2} + \frac{1}{3} \frac{\rho_0^2}{C_0} \frac{\partial^2 C_0}{\partial \rho_0^2} + \frac{1}{2} (u+1)(8u+5)\alpha \right\} , \quad \omega_s \tau \gg 1 ,$$

$$(7.2)$$

Since the normal fluid density is given by Eqs. (5.13) and (5.14) in both frequency regions, the leading term for the first sound increases as T^3 , in striking contrast to the $T^4 \ln T^{-1}$ increase of bulk liquid ^4He . The absence of the logarithmic term in two dimensions stems from the angle integrals. Figure 7 illustrates the temperature variation of the first sound velocity in both frequency regions at very low and moderately low temperatures. In the region above about $T \sim 0.9$ K, the sound velocity decreases due to $\alpha(\beta, z)$. We can confirm that the phonon excitation spectrum is strongly anomalous, and the first sound velocity in the hydrodynamic region increases more than in the collision

region. In this plot, the parameters u and $(\rho_o^3/C_o)(\partial^2 C_o/\partial \rho_o^2)$ are taken to be 1.8 and 0.19, respectively, as used by Singh-Prakash²⁸ and Maris.²⁹ The corresponding attenuation coefficients in Eqs. (6.10) and (6.16) are given by

$$\alpha_1(T) = \begin{cases} \frac{\omega_s r}{8} \left[(2u^2 + 3u + 1) \frac{\rho_n}{\rho_o} - \frac{1}{4}(2\alpha + \beta) \right] , & \omega_s r \ll 1 \end{cases} \quad (7.3)$$

$$\begin{cases} \frac{1}{2\omega_s r} \left[\frac{1}{8}(6\alpha + 3\beta) + (u+1) \frac{\rho_n}{\rho_o} \right] , & \omega_s r \gg 1 \end{cases} \quad (7.4)$$

The second sound and corresponding attenuation coefficients given in Eqs. (6.12), (6.13), (6.18) and (6.19) can be expressed as follows:

$$C_2(T) = \frac{C_o}{\sqrt{2}} \left[1 - \frac{1}{2} \left(\beta + 2u^2 \frac{\rho_n}{\rho_o} \right) \right] \left[1 + \frac{1}{2} (2\alpha + \beta) - (u+1) \frac{\rho_n}{\rho_o} \right] . \quad (7.5)$$

$$C_2(T) = \frac{C_2}{\sqrt{2}} \left[1 - (\alpha + (u+1)^2 \frac{\rho_n}{\rho_o} + \frac{1}{2}\beta) + \alpha \right] \left[1 - \frac{1}{2}\beta - u^2 \frac{\rho_n}{\rho_o} \right] , \quad (7.6)$$

$$\alpha(T) = \begin{cases} \frac{\omega_s^2 r}{8C_o} \left[1 + (7u^2 + 4u + 1) \frac{\rho_n}{\rho_o} \right] , & \omega_s r \ll 1 , \end{cases} \quad (7.7)$$

$$\begin{cases} \frac{1}{6\omega_s r} \left[1 + \frac{1}{3} \left(11u^2 - 6 + \frac{2\rho_o^2}{C_o} \frac{\partial^2 C_o}{\partial \rho_o^2} \right) \frac{\rho_n}{\rho_o} - 2(\alpha' + \gamma P_T^2 - 5\delta P_T^4) \right] , \end{cases}$$

$$\omega_s r \gg 1 , \quad (7.8)$$

The attenuation coefficients $\alpha_1(T)$ and $\alpha_2(T)$ in both regions show the variation with $\rho_n(T)$ under the assumption of constant r . This result is similar to the bulk case.⁵² However, $\alpha_1(T)$ in the hydrodynamic region and $\alpha_2(T)$ in the

collisionless region at temperatures above ~ 0.6 K will depend not only on $\rho_n(T)$ but also moderately on $\alpha(\beta, Z)$ and β [Eq. (6.14)].

Figures 8 and 9 represent our theoretical results for the temperature variations of the first and second sounds at low frequencies, respectively. We find that at absolute zero, the second sound velocity C_2 is about $1/\sqrt{2}$ of the first sound velocity. As temperature increases above ~ 0.8 K, the contribution of $\alpha(\beta, Z)$ to the first sound velocity is significant, causing a dramatic decrease in the velocity.

We note in Figure 9 that as temperature increases, the second sound passes through a gentle maximum, reaches a minimum at about 0.6 K, and then arrives at another moderate plateau. After this it decreases rapidly. However, the effect of $\alpha(\beta, Z)$ on the second sound, which is different from that of the first sound, is a slight increase of the velocity on the plateau.

In order to fit the data of the third sound corresponding to an atomic coverage of $D = 1.77$, we have adopted the following potential and roton parameters:

$$a = 2.55 \text{ \AA} , \quad E_0 = 0.12 \text{ K} , \quad V_0 = 2.17 \text{ K} , \quad q_0 = 0.73 \text{ \AA} ,$$

$$\Delta = 2.80 \text{ K} , \quad m^* = 2.04 m .$$

These parameters are slightly different from those we have taken in Ref. 17, which is due to $\alpha(\beta, z)$. In Figure 10, we show that our microscopic approach reproduces the temperature variation of third sound velocity. Our expression Eq. (6.22) is very similar to the result given by Rutledge et al,⁵³ who obtained a T^3 term [see their Eq. (29)] with a temperature-dependent coefficient. However, the coefficient X_1 of the T^3 term in Eq. (6.22) contains the potential

parameters as well as being temperature dependent, and we have also obtained higher-order terms, such as T^5 and roton terms. Therefore, our derivation is more meaningful and should fit the data more accurately.

In conclusion, we have evaluated the temperature variation of the elementary excitation spectrum of thin liquid ^4He films within the ring diagram approximation. The effect of temperature on the phonon spectrum is very small for very low temperatures, and thus three-phonon processes do not play much of a role. However, as temperature increases from 0.6 K to the vicinity of the two-dimensional transition temperature $T_\lambda = 1.21$ K, the temperature effect is very significant for the physical quantities of thin liquid ^4He films as in bulk liquid ^4He .

Acknowledgments

This work was supported by the Basic Science Institute Program, Ministry of Education, Republic of Korea, 1990, the Center for Thermal and Statistical Physics, 1991, and the U.S. Office of Naval Research.

Appendix A: Derivation of Eq. (3.7)

Substituting Eqs. (3.4) and (3.5) into Eq. (3.6) and retaining just the first term, we have

$$\text{First Term} = \frac{1}{\beta n} \sum_j \frac{\frac{2nq^2}{q^4 + (2\pi j/\beta)^2} - \frac{n\alpha q^4}{[q^4 + (2\pi h/\beta)^2]^2}}{1 + U(q) \left\{ \frac{2nq^2}{q^4 + (\frac{2\pi j}{\beta})^2} - \frac{n\alpha q^4}{[q^4 + (\frac{2\pi j}{\beta})^2]^2} \right\}} \quad (\text{A.1})$$

where $\alpha = 12\gamma(z)/\beta$. We can rewrite this equation in two parts as

$$\begin{aligned} \text{First Term} = & \frac{q^2}{\beta} \sum_j \frac{1 + \frac{2nu + \alpha}{2[(nu)^2 + nu\alpha]^{\frac{1}{2}}}}{q^4 + nuq^2 + q^2[(nu)^2 + nu\alpha]^{\frac{1}{2}} + (\frac{2\pi j}{\beta})^2} \\ & + \frac{q^2}{\beta} \sum_j \frac{1 - \frac{2nu + \alpha}{2[(nu)^2 + nu\alpha]^{\frac{1}{2}}}}{q^4 + nuq^2 - q^2[(nu)^2 + nu\alpha]^{\frac{1}{2}} + (\frac{2\pi j}{\beta})^2} \quad (\text{A.2}) \end{aligned}$$

Using the summation formula

$$\sum_{j=-\infty}^{\infty} \frac{1}{x^2 + j^2} = \frac{\pi}{x} \coth(\pi x) \quad (\text{A.3})$$

the first term of Eq. (A.2) becomes

$$\frac{q \coth(\frac{1}{2}\beta q) [q^2 + U_+]^{\frac{1}{2}}}{2[q^2 + U_+]^{\frac{1}{2}}} \left\{ 1 + \frac{2nu + \alpha}{2[(nu)^2 + nu\alpha]^{\frac{1}{2}}} \right\} \quad (\text{A.4})$$

where $U_+ = nu[1 + (1 + \alpha/nu)^{1/2}]$. Through a similar calculation for the second terms in (A.1) and (A.2) and making use of the summation formula

$$\sum_{j=-\infty}^{\infty} \frac{1}{(1+m^2 j^2)^2} = \frac{\pi^2}{2m^2} \operatorname{cosech}^2\left(\frac{\pi}{m}\right) + \frac{\pi}{2m} \coth\left(\frac{\pi}{m}\right) , \quad (\text{A.5})$$

we then obtain Eq. (3.7).

Appendix B: Numerical evaluation of $\gamma(z)$

The total number of particles of the system is determined by integrating the distribution function together with the two-dimensional density of states,

$$N = A \frac{2\pi m}{h^2} \int \frac{dE}{e^{\beta(E-\mu)} - 1}, \quad (B.1)$$

where μ is the chemical potential. Expanding the denominator of Eq. (B.1) and performing the integration over energy, we obtain the simple form

$$\frac{\mu}{k_B T} = \ln[1 - e^{-\theta}] \quad , \quad (B.2)$$

where we have used the relations

$$\sum_j \frac{1}{j} e^{j\mu/k_B T} = -\ln[1 - e^{-\mu/k_B T}] \quad , \quad \theta = \left(\frac{N h^2}{A 2\pi m k_B T} \right) \quad .$$

For sufficiently low temperatures, i.e., $\theta \gg 1$, Eq. (B.2) can be expressed as

$$\frac{\mu}{k_B T} = -\frac{1}{n} e^{-n\theta} \quad . \quad (B.3)$$

At a density of $2.79 \times 10^{-2} \text{ \AA}^2$, the numerical value of θ is $2.124/T$, and we can make the approximation $z \approx 1 - \exp[-2.12/T]$ for $\theta > 1$ ($T > 2.12 \text{ K}$). Therefore, $G_1(z)$ can be expressed approximately as

$$G_1(z) = \sum_{\ell=1}^{\infty} \frac{z^\ell}{\ell} = -\ln(1-z) \approx \frac{2.12}{T} \quad . \quad (B.4)$$

On the other hand, we can write $G_2(z)$ as

$$G_2(z) = \int \frac{d}{dz} \sum_{\ell=1}^{\infty} \frac{z^{\ell}}{\ell^2} dz = - \int dz \frac{1}{z} \ln(1-z) \quad . \quad (\text{B.5})$$

However, this function can not be expressed as a finite combination of elementary functions.⁴⁵ Therefore, for $\gamma(z)$ we must perform the numerical calculation.

References

1. L. D. Landau, J. Phys. (Moscow) 11, 91 (1947).
2. N. N. Bogoliubov, J. Phys. (Moscow) 11, 23 (1947).
3. R. P. Feynman and M. Cohen, Phys. Rev. 102, 1189 (1956).
4. T. D. Lee and C. N. Yang, Phys. Rev. 113, 1403 (1959); 117, 897 (1960).
5. T. Samulski and A. Isihara, Physica 86A, 257 (1977); Phys. Rev. B 16, 1969 (1977); C. J. Nisteruk and A. Isihara Phys. Rev. 154, 1150 (1967).
6. T. Kebukawa, S. Yamasaki and S. Sunakawa, Prog. Theor. Phys. 49, 1802 (1973); F. Iwamoto, Prog. Theor. Phys. 44, 1121 (1970).
7. H. J. Maris, Rev. Mod. Phys. 49, 341 (1977).
8. S. A. Chin and E. Krotscheck, Phys. Rev. Lett. 65, 2658 (1990).
9. M. V. Rama Krishna and K. B. Whaley, Phys. Rev. Lett. 64, 1126 (1990).
10. T. Chakraborty, A. Kallio and M. Puoskari, Phys. Rev. B 33, 635 (1986); E. C. Svensson, V. A. Sears, A. D. B. Woods and P. Martel, Phys. Rev. B. 21, 3638 (1980).
11. G. K. S. Wong, P. A. Crowell, H. A. Cho and J. D. Reppy, Phys. Rev. Lett. 65, 2410 (1990); M. Kriss and I. Rudnick, J. Low Temp. Phys. 3, 339 (1970); D. Finotello, K. A. Gillis, A. Wong and M. H. W. Chan, Phys. Rev. Lett. 61, 1954 (1988).
12. W. G. Stirling and H. R. Glyde, Phys. Rev. B 41, 4224 (1990).
13. A. Isihara and C. I. Um, Phys. Rev. B 19, 5725 (1979); A. Isihara, S. T. Choh, W. H. Kahng and C. I. Um, Physica 100B, 74 (1980).
14. K. H. Oh, C. I. Um, W. H. Kahng and A. Isihara, Phys. Rev. B 33, 7550 (1986).
15. C. I. Um, W. H. Kahng, K. H. Yeon, S. T. Choh and A. Isihara, Phys. Rev. B 29, 5203 (1984).
16. H. G. Oh, C. I. Um and A. Isihara, Phys. Rev. B 34, 6151 (1986).

17. A. Isihara, C. I. Um, W. H. Kahng, H. G. Oh and S. T. Choh, Phys. Rev. B 28, 2509 (1983).
18. A. Isihara, C. I. Um, C. W. Chun, W. H. Kahng and S. T. Choh, Jpn. J. Appl. Phys. 26, Suppl. 26-3, 297 (1987); C. I. Um and C. W. Jun, J. Korean Phys. Soc. 20, 180 (1987).
19. C. I. Um, C. W. Jun, W. H. Kahng and T. F. George, Phys. Rev. B 38, 8838 (1988); C. I. Um and C. W. Jun, J. Korean Phys. Soc. 21, 41, 51, 209 (1988).
20. C. I. Um, C. W. Jun, W. H. Kahng and T. F. George, Phys. Rev. B 38, 8834 (1988); C. I. Um, C. W. Jun, J. Korean Phys. Soc. 21, 213 (1988); C. I. Um, C. W. Jun, W. H. Kahng and A. Isihara, Jpn. J. Appl. Phys. 26, Suppl. 26-3, 295 (1987).
21. C. I. Um, C. W. Jun, H. J. Shin and T. F. George, J. Low Temp. Phys. 78, 51 (1990); C. I. Um, C. W. Jun and H. J. Shin, J. Korean Phys. Soc. 21, 372 (1989).
22. A. B. D. Wood, Phys. Rev. Lett. 12, 69 (1964).
23. B. Hallock, Phys. Rev. A 5, 320 (1972); O. W. Dietrich, C. H. Huang and C. Passal, Phys. Rev. A 5, 1377 (1972).
24. A. Isihara, Prog. Theor. Phys. Suppl. 44, 1 (1969).
25. N. N. Bogoliubov and D. N. Zubarev, Zh. Eksp. Teor. Fiz. 28, 129 (1955) [Sov. Phys.-JETP 1, 83 (1955)].
26. P. C. Hohenberg and P. C. Martin, Phys. Rev. Lett. 12, 69 (1964); T. Morita and H. Hara, Prog. Theor. Phys. 41, 60 (1969).
27. A. Andreev and I. M. Khalatnikov, Zh. Eksp. Teor. Fiz. 44, 2053 (1963) [Sov. Phys.-JETP 17, 1384 (1963)].
28. K. K. Singh and J. Prakash, Phys. Rev. B 17, 1523 (1978); K. K. Singh, *ibid.* 29, 5203 (1984).

29. H. J. Maris and W. E. Massey, Phys. Rev. Lett. 25, 220 (1970); H. J. Maris, Phys. Rev. A 9, 1412 (1974).
30. Y. Disatnik, Phys. Rev. Lett. 31, 277 (1972).
31. I. Rudnick, R. S. Kagiwada, J. C. Fraser and E. Guyon, Phys. Rev. Lett. 20, 430 (1968); J. S. Brooks, F. M. Ellis and R. B. Hallock, Phys. Rev. Lett. 40, 240 (1978); J. A. Roth, G. J. Jelatis and J. D. Maynard, Phys. Rev. Lett. 44, 333 (1980).
32. J. E. Rutledge, W. L. MacMillan, J. M. Mochel and T. E. Washburn, Phys. Rev. B 18, 2155 (1978); T. E. Washburn, J. E. Rutledge and J. M. Mochel, in *Low Temperature Physics-Lt-14*, Vol. 1, edited by M. Krusis and M. Vuorio (North-Holland, Amsterdam, 1975), p. 372 ff.
33. W. G. Stirling, J. Phys. (Paris), Colloq. C6, 39, 1334 (1978).
34. R. C. Dynes and V. Narayanamurti, Phys. Rev. B 12, 1720 (1975); W. R. Junker and C. Elbaum, Phys. Rev. B 15, 162 (1977).
35. N. E. Phillips, C. G. Waterfield and J. K. Hoffer, Phys. Rev. Lett. 25, 1260 (1970).
36. D. S. Greywall, Phys. Rev. B 18, 2127 (1978).
37. C. I. Um and Y. B. Kang, J. Korean Phys. Soc. 19, 287 (1986).
38. M. Bretz and J. G. Dash, Phys. Rev. Lett. 26, 963 (1971); 27, 647 (1971); M. Bretz, J. G. Dash and G. B. Huff, Phys. Rev. Lett. 28, 729 (1972); D. F. Brewer, J. Low Temp. Phys. 3, 205 (1970); D. L. Goodstein and J. D. Dash, Phys. Rev. 168, 249 (1968).
39. M. Bretz, J. G. Dash, D. C. Hickernell, E. D. Mclean and O. E. Vilches, Phys. Rev. A 8, 1589 (1973).
40. E. Krotscheck, Phys. Rev. B 32, 5713 (1985).
41. R. A. Aziz, V. P. S. Nain, J. C. Carley, W. L. Taylor and G. T. McConville, J. Chem. Phys. 70, 4330 (1979).

42. J. DuPont-Roc, as quoted in Ref. 45.
43. A. Isihara, S. T. Choh and C. I. Um, Phys. Rev. B 20, 4482 (1979).
44. D. J. Bishop and J. D. Reppy, Phys. Rev. Lett. 40, 1727 (1978).
45. Gradshteyn and Ryzhik, *Table of Integrals Series and Products* (Academic, New York, 1965).
46. G. Senger, M. L. Ristig, K. E. Kürten and C. E. Campbell, Phys Rev. B 33, 7562 (1986).
47. P. J. Bendt, R. D. Cowan and J. L. Yarnell, Phys. Rev. 113, 1386 (1959).
48. P. Suebka and P. Lu, Phys. Rev. B 31, 1603 (1985).
49. K. A. Brueckner and K. Swada, Phys. Rev. 106, 1128 (1957).
50. C. E. Campbell, K. E. Kürten, M. L. Listig and G. Senger, Phys. Rev. B 30, 3728 (1984).
51. R. A. Cowley and A. D. B. Woods, Can. J. Phys. 49, 177 (1971).
52. K. H. Bennemann and J. B. Ketterson, *The Physics of Liquid and Solid Helium* (Wiley, New York, 1976), Part 1, Chap. 1.
53. J. E. Rutledge, W. L. McMillen, J. M. Mochel and T. E. Washburn, Phys. Rev. B 18, 2155 (1978).

Table I. Potential and roton parameters to fit the experimental data of specific heat in the microscopic theory presented in this paper.

$n(1/\text{\AA}^2)$	$a(\text{\AA})$	$V_o(\kappa)$	$E_o(\kappa)$	$q_o(\text{\AA}^{-1})$	m^*/m	$\Delta(k)$
0.0273	3.565	9.331	8.005	0.875 ± 0.275	2.027	3.29
0.0279	3.581	8.369	7.140	0.814 ± 0.302	2.042	3.35
0.0399	3.161	9.297	7.943	0.92 ± 0.350	2.184	4.00
0.0419	3.295	8.040	6.820	0.90 ± 0.320	1.891	4.30

Table II. Numerical values of $\gamma(z) = G_2(z)/G_1(z)$ versus T.

T	$G_1(z) = \frac{2.12}{T}$	$G_2(z)$	$\gamma(z) = G_2(z)/G_1(z)$
0.0714	29.6918	1.6449	0.0554
0.1732	12.2401	1.6448	0.1343
0.2357	8.9944	1.6436	0.1827
0.2857	7.4203	1.6398	0.2209
0.3286	6.4516	1.6331	0.2531
0.3895	5.4428	1.6169	0.2970
0.4393	4.8258	1.5980	0.3311
0.4507	4.7037	1.5930	0.3386
0.5000	4.2400	1.5689	0.3700
0.5571	3.8054	1.5369	0.4038
0.6571	3.2262	1.4741	0.4569
0.6893	3.0755	1.4528	0.4723
0.7321	2.8957	1.4242	0.4918
0.7750	2.7354	1.3955	0.5101
0.8571	2.4734	1.3409	0.5421
0.8940	2.3713	1.3169	0.5553
0.9643	2.1984	1.2721	0.5786
1.0914	1.9424	1.1955	0.6154
1.1634	1.8222	1.1548	0.6337
1.2120	1.7491	1.1286	0.6452
1.2720	1.6666	1.0974	0.6584
1.3790	1.5373	1.0451	0.6798
1.4450	1.4671	1.0149	0.6919
1.5150	1.3993	0.9844	0.7035

Figure captions

- Figure 1. Specific heat of ^4He films plotted against temperature. The solid, dashed, dotted and dash-dotted lines represent the theoretical calculations, and the experimental data are represented by +, x, o and Δ .
- Figure 2. Theoretical excitation spectrums of the ^4He films deduced from the specific data as a function of the dimensionless parameter qa .
- Figure 3. Structure factor $S(q)$ deduced from the excitation spectrum as a function of the wave vector q .
- Figure 4. Temperature variation of $\gamma(z)$.
- Figure 5. Temperature variation of the excitation spectrum.
- Figure 6. Temperature variation of the structure factor deduced from the excitation spectrum in Figure 5.
- Figure 7. First sound velocities in the hydrodynamic ($\omega_s \tau \ll 1$) and collisionless regions ($\omega_s \tau \gg 1$). The dashed lines are the velocities when $\alpha(\beta, z)$ is taken into account in both regions.
- Figure 8. First sound velocity versus temperature. The dashed line is due to the effect of $\alpha(\beta, z)$.
- Figure 9. Second sound velocity versus temperature. The dashed line is due to the effect of $\alpha(\beta, z)$.
- Figure 10. Third sound velocity for $D = 1.77$ as a function of temperature, where the circles are data from Rutledge et al, and the solid curve is the present theory.

Fig. 1

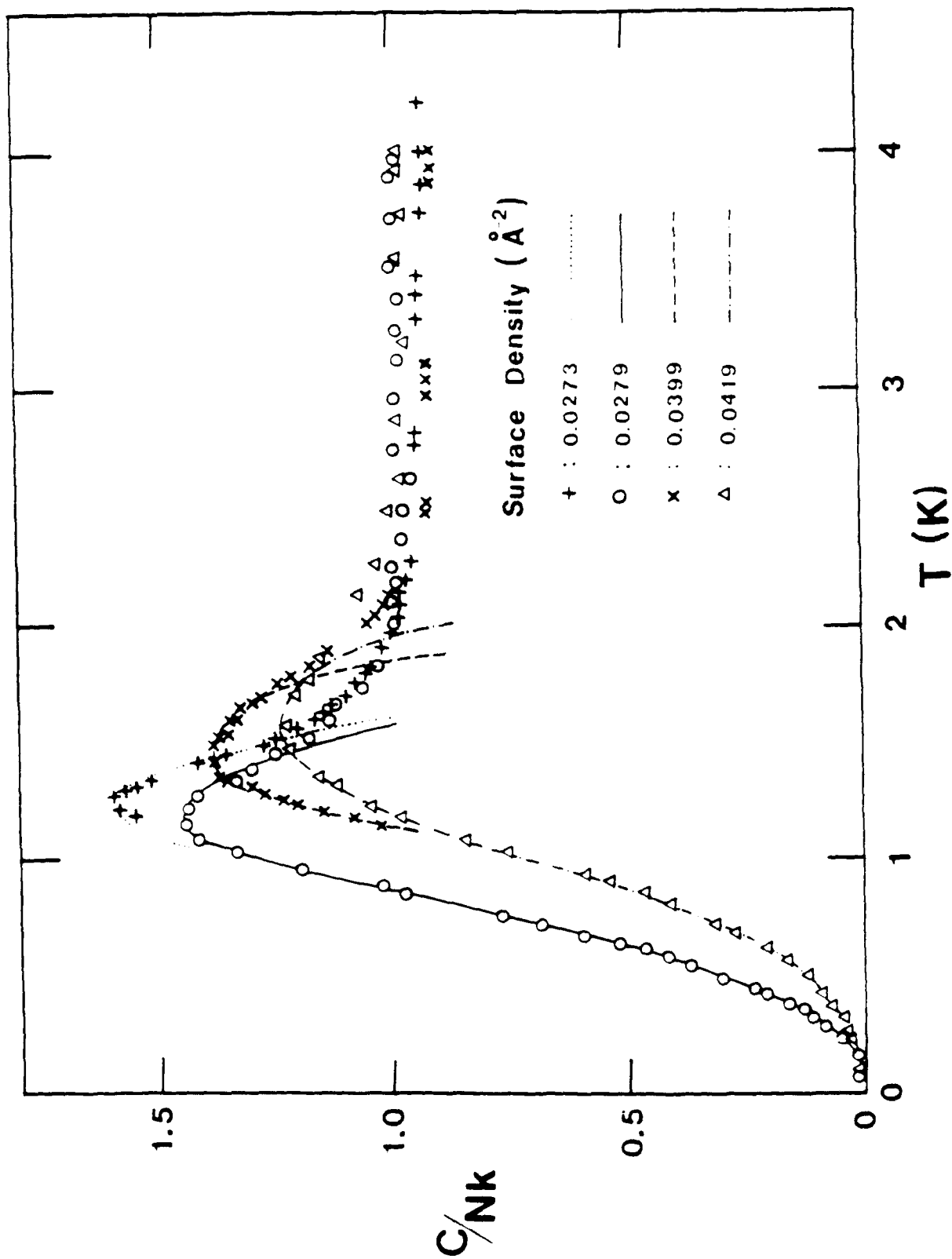


Fig. 2

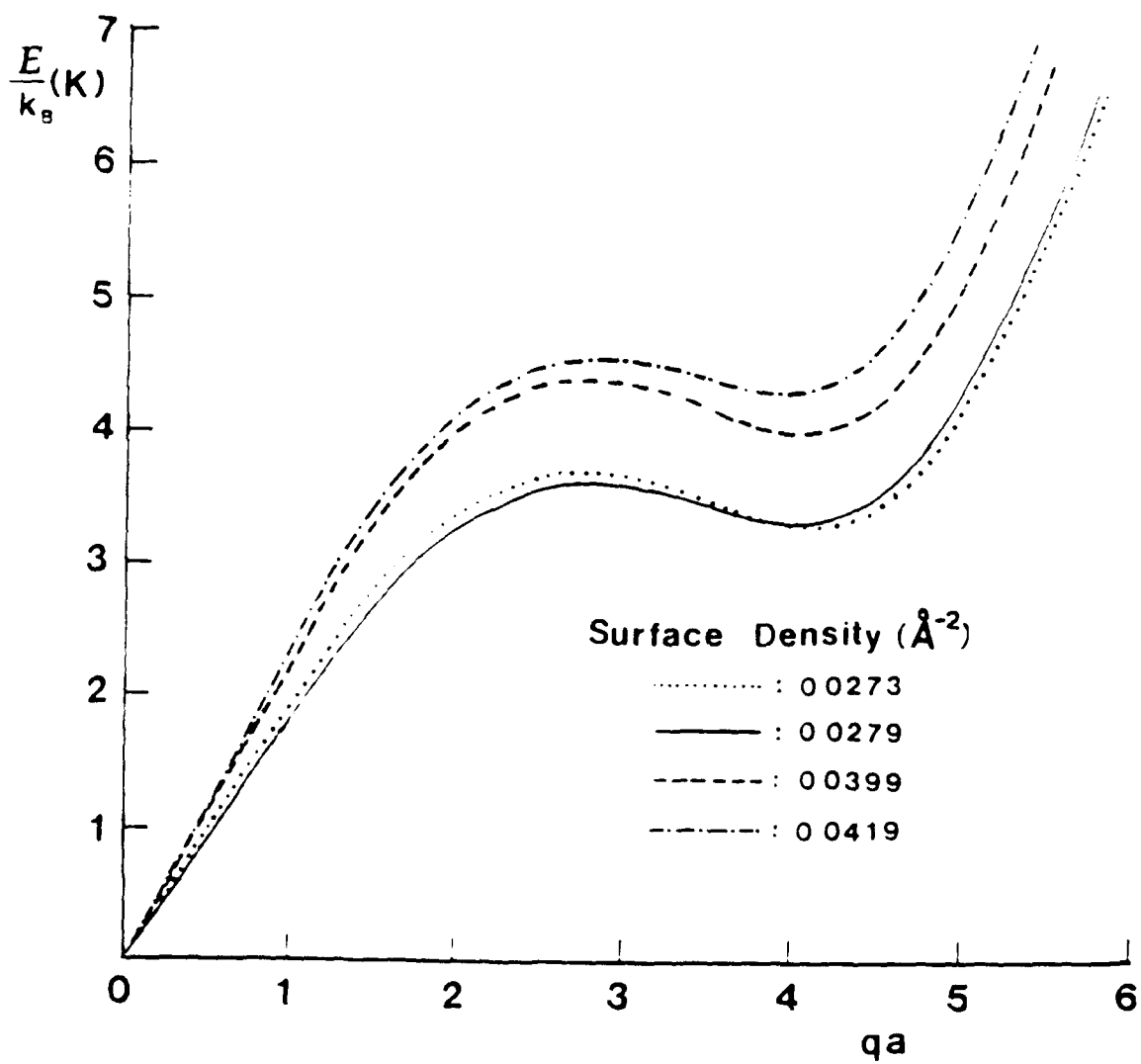


Fig. 3

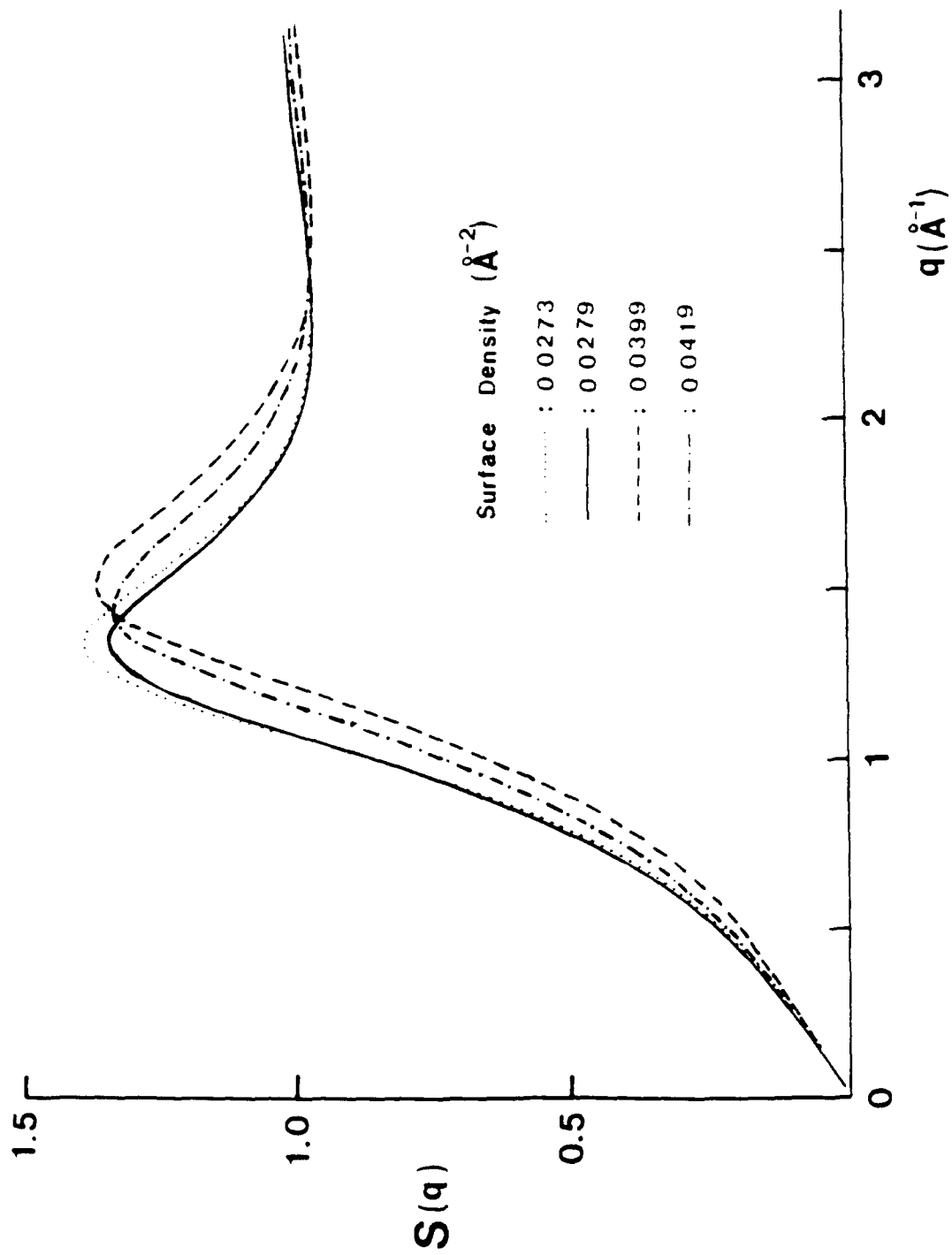
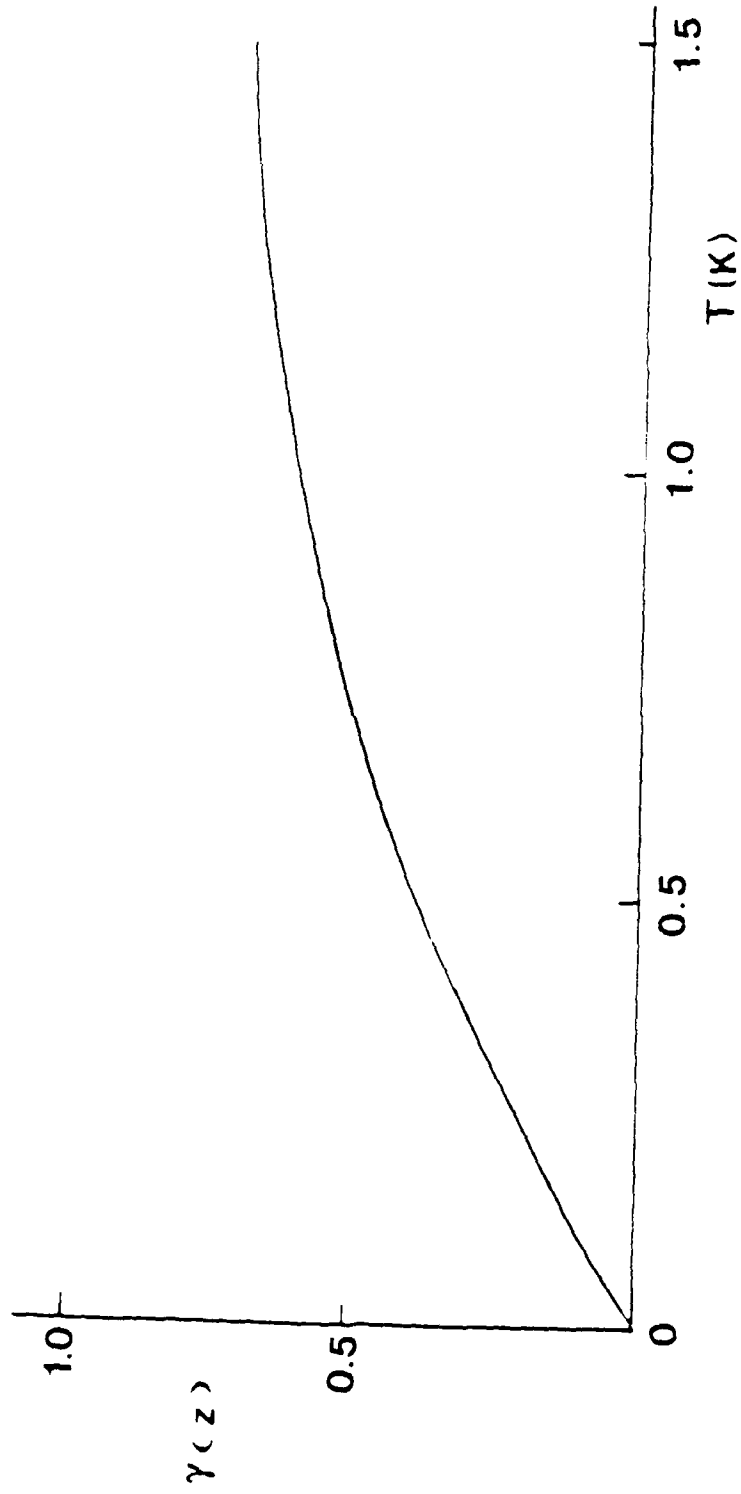


Fig. 4



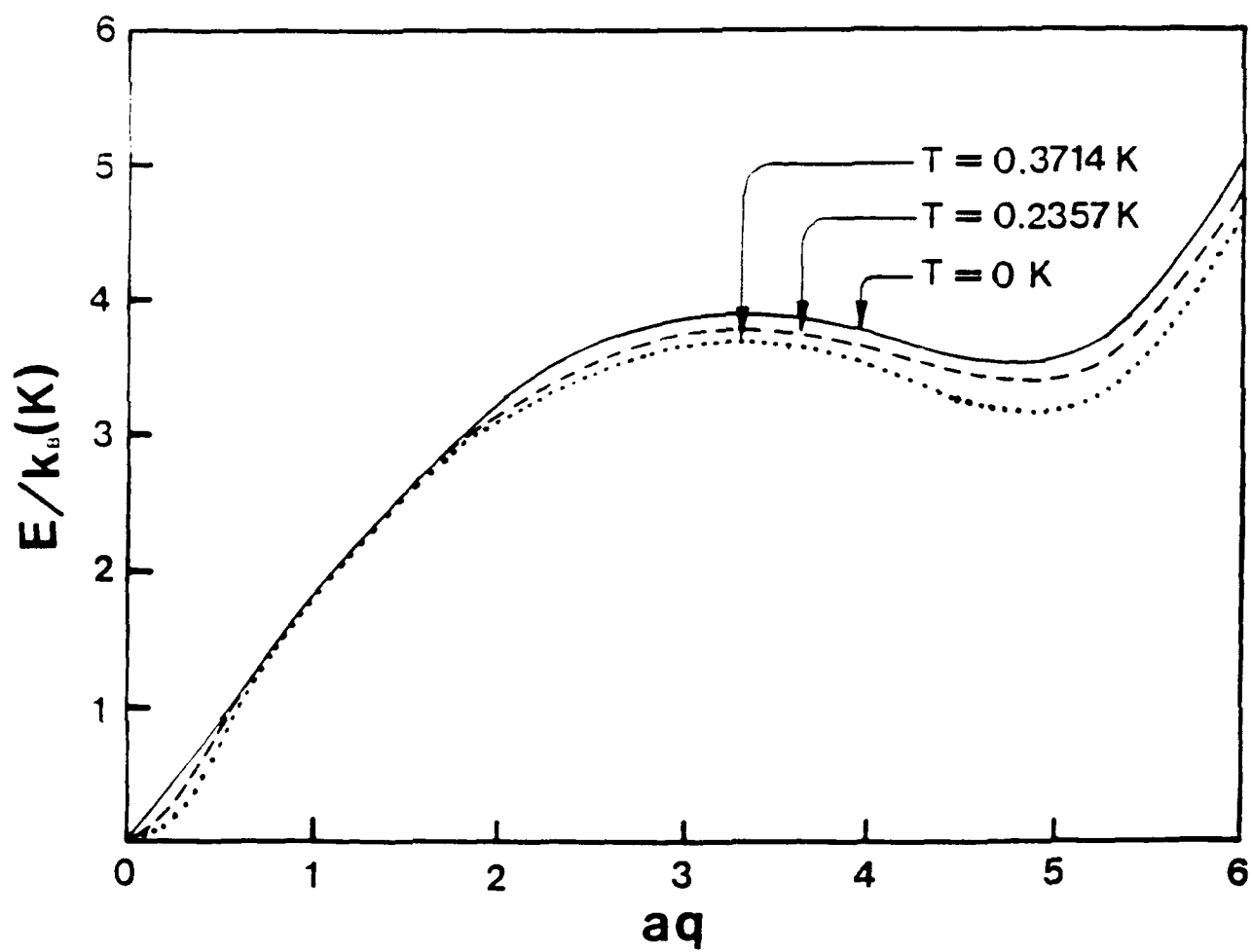


Fig. 6

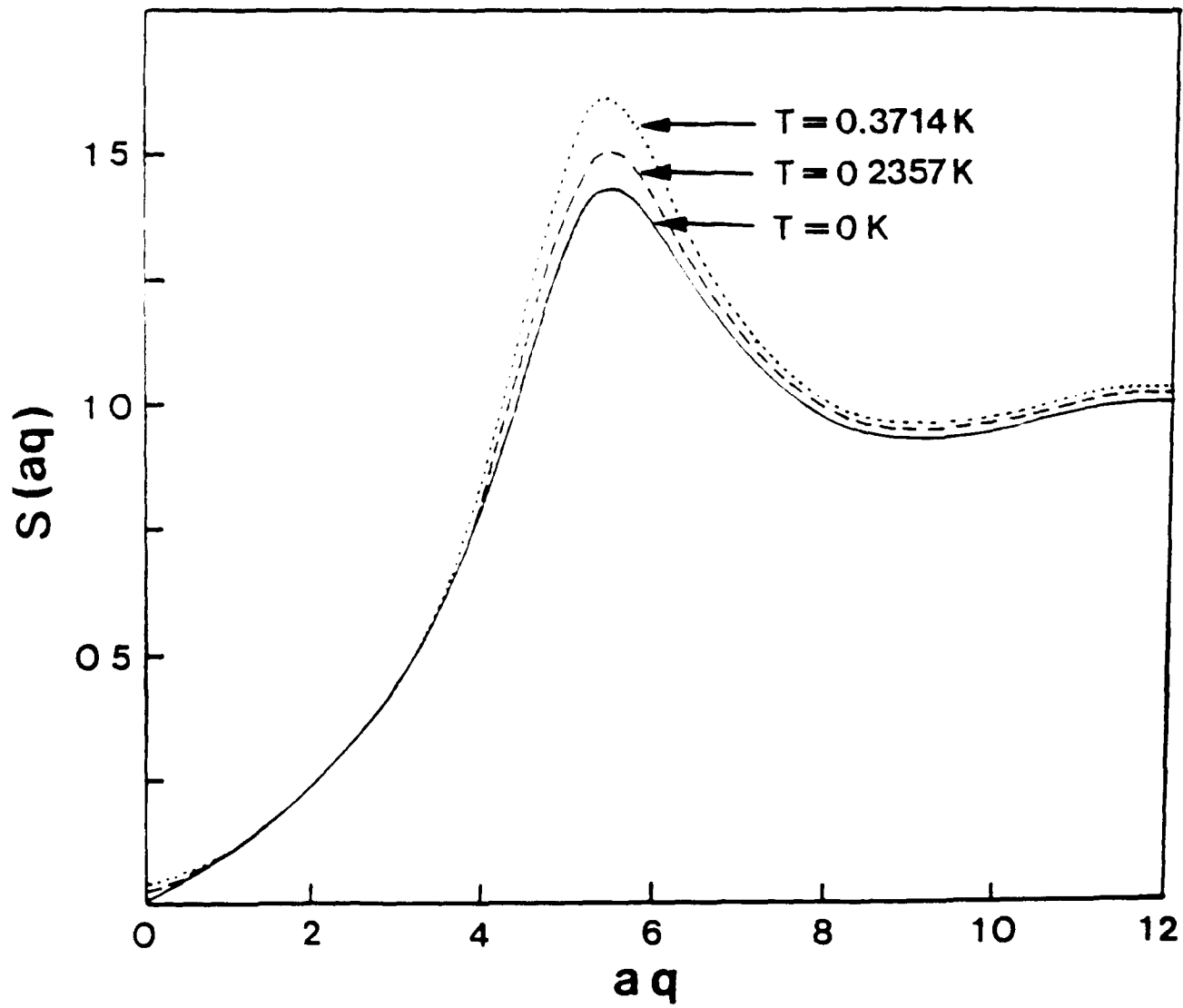


Fig. 7

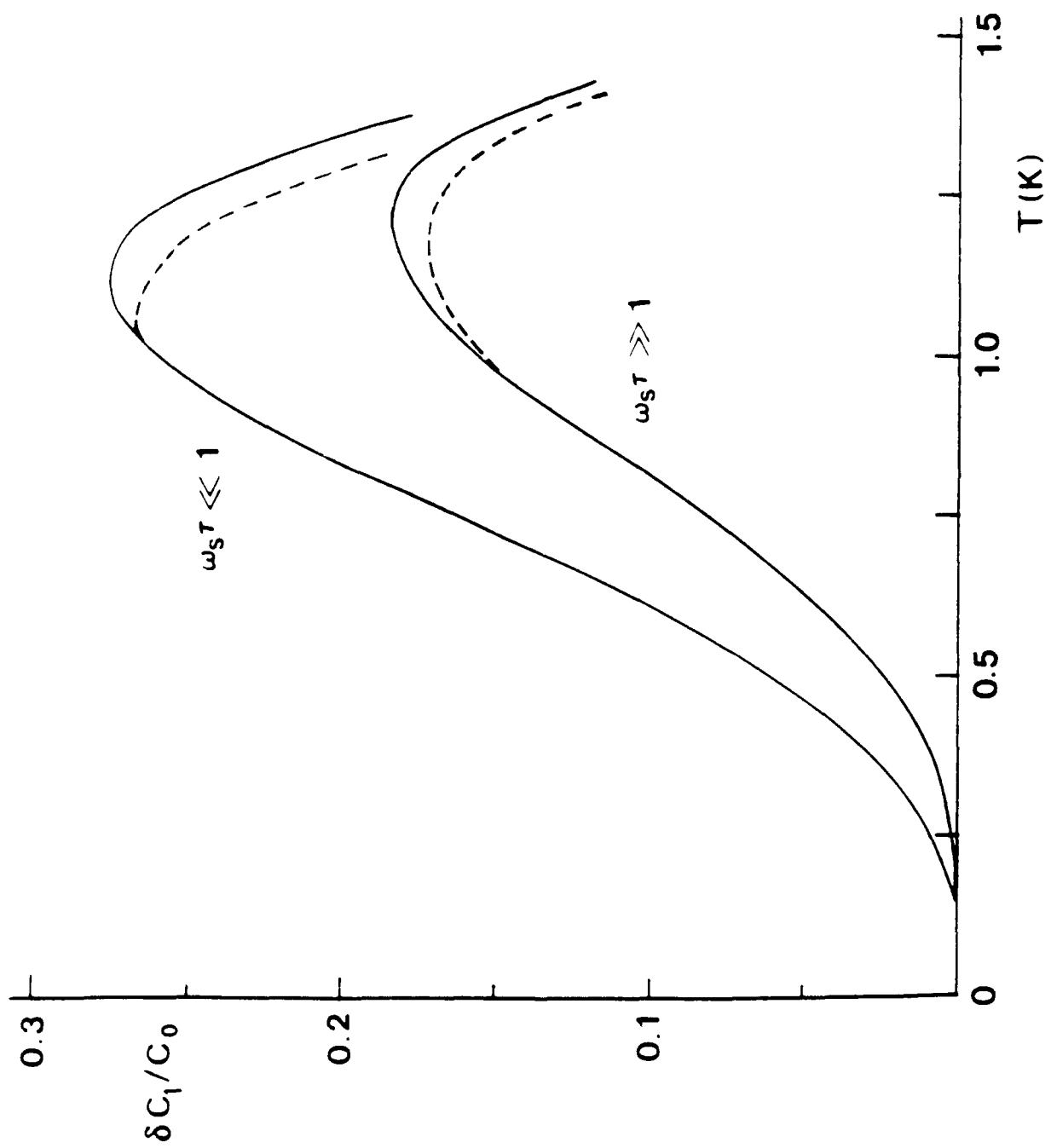


Fig. 8

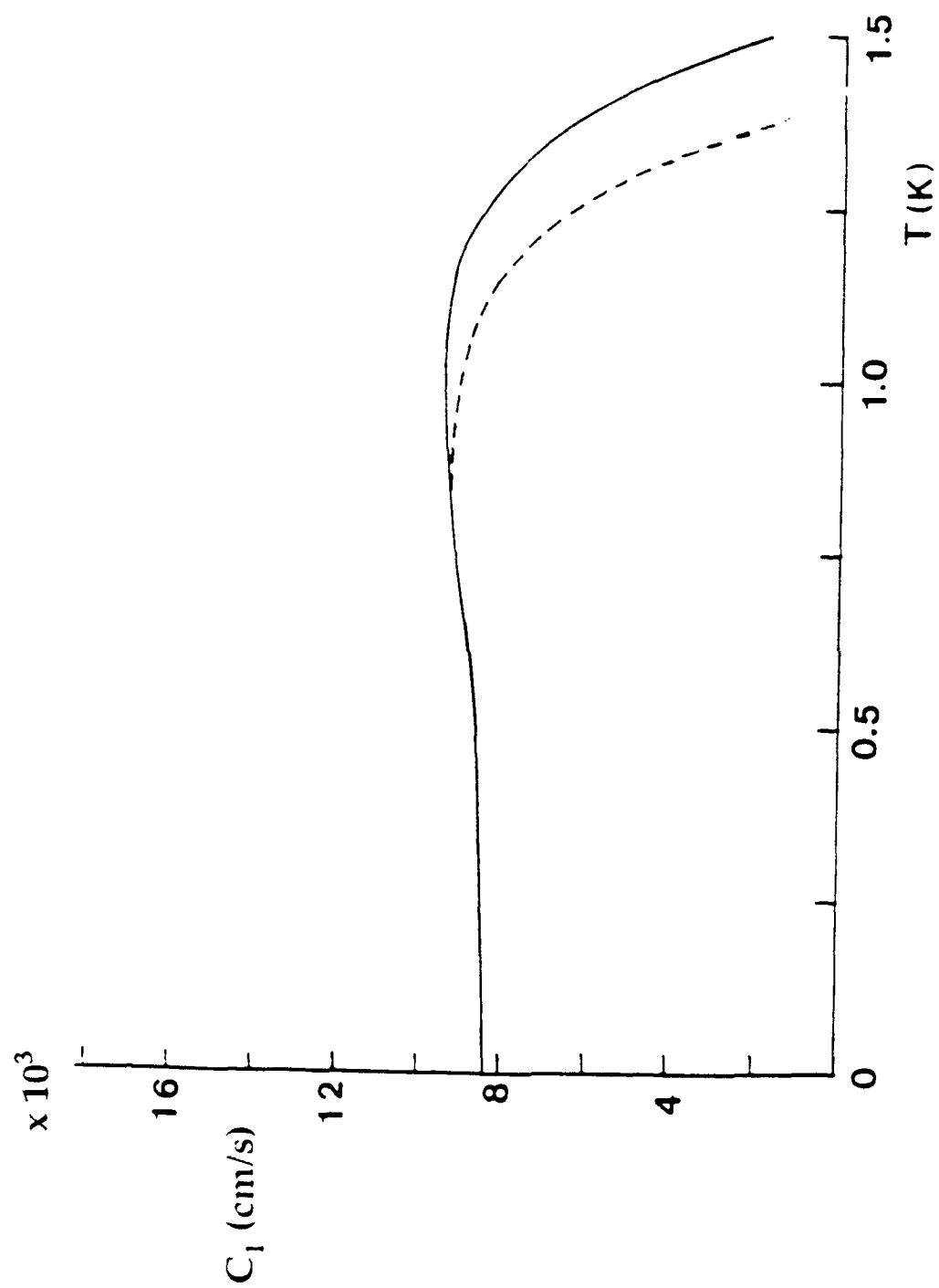


Fig. 9

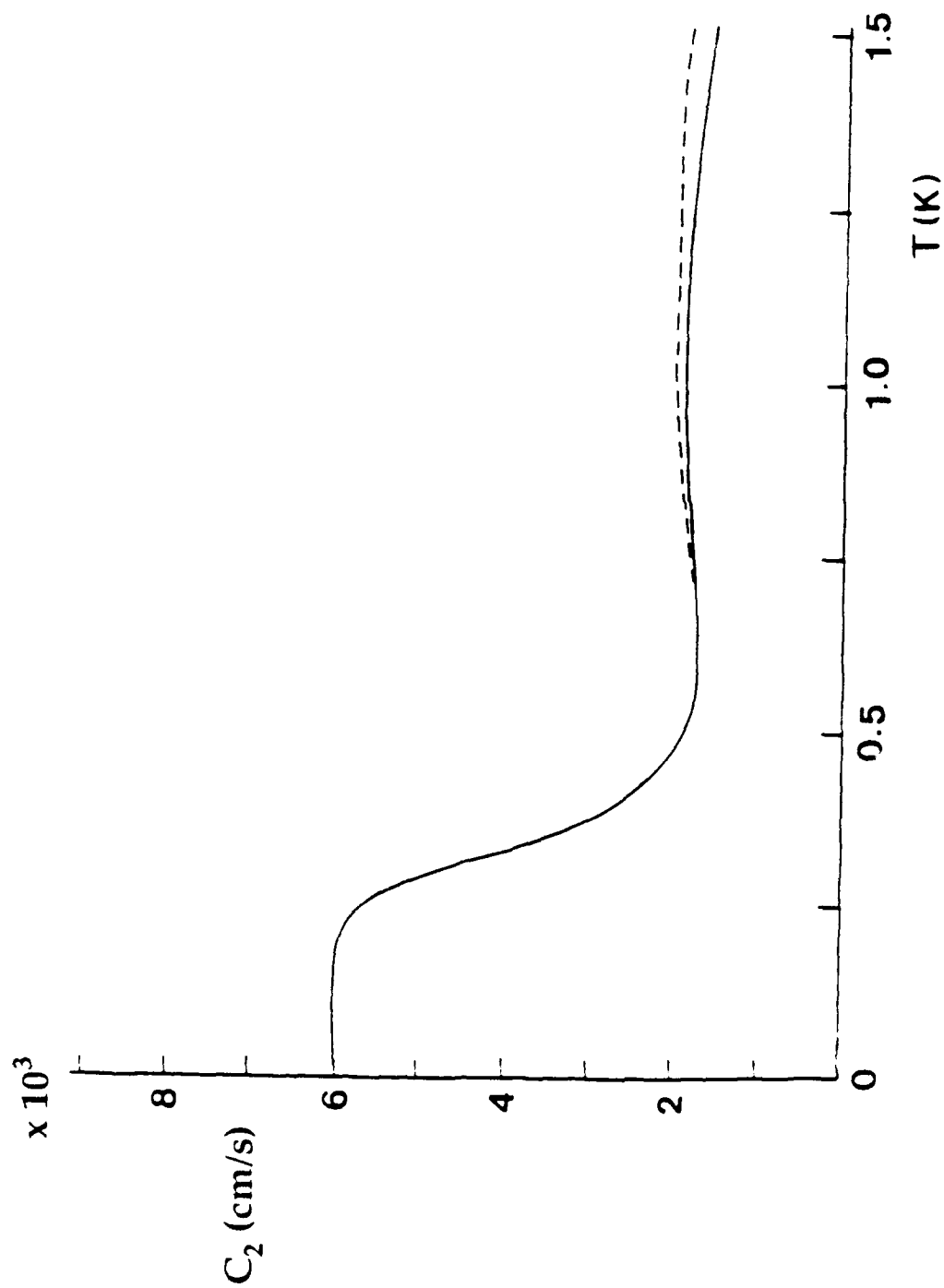


Fig. 10

